Meteoritics & Planetary Science 33, 999–1016 (1998)

Orbital and temporal distributions of meteorites originating in the asteroid belt

ALESSANDRO MORBIDELLI[1]* AND BRETT GLADMAN[1,2]

[1]Observatoire de Nice, B.P. 4229, 06304 Nice Cedex 4, France
[2]Canadian Institute for Theoretical Astrophysics, University of Toronto, Toronto, Ontario, M5S 3H8, Canada
*Correspondence author's e-mail address: morby@obs-nice.fr

(Received 1997 July 29; accepted in revised form 1998 May 13)

We dedicate this paper to our friend and colleague Fabio Migliorini.

Abstract–The recent discovery of the importance of Sun-grazing phenomena dramatically changed our understanding of the dynamics of objects emerging from the asteroid belt *via* resonant phenomena. The typical lifetimes of such objects are now expected to be <10 Ma, thus demanding a reassessment of our general picture of the meteorite delivery process. By analysing direct numerical integrations of ~2000 test particles beginning in the ν_6, 3:1, and 5:2 resonances in the main belt, we have reexamined the orbital and temporal distribution of meteoroids that journey to Earth. Comparing the results with fireball data, we find that the orbital distribution of Earth-impacting chondrites is consistent with a steady-state injection of meteoroids into the 3:1 and ν_6 resonances. Because this is the most complete and unbiased data set concerning Earth-impacting meteoroids, the agreement leads us to believe that our model is accurate. The simulations predict a P.M. fall ratio for chondrites ~14% lower than the observed value of ~68%, which argues for a moderate bias being present in this statistic. Most interestingly, the typical meteorite transfer times predicted by our models are several factors lower than the typical chondrite exposure ages, which implies that these meteorites acquired most of their exposure in the main belt before entering the resonances. We discuss some processes that would allow such preexposure. The case of achondrites and iron meteorites is also briefly discussed.

INTRODUCTION

Decades ago, an asteroidal source of chondrites was problematic since there was no understanding of a process that was capable of modifying the orbits of fragments produced in the main belt into Earth-crossing orbits in a manner sufficient to supply the observed flux. A direct modification of a circular orbit at $a = 2$ AU requires a velocity change of ≃4 km/s to reach an Earth-crossing orbit, which is much in excess of what is generally regarded as typical ejection velocities in fragmentation events during asteroid collisions. Even if only Mars crossing needed to be achieved, with subsequent Martian close encounters being responsible for finally delivering objects to Earth-crossing orbits, the efficiency seemed so low that a cometary source for the chondrites was explored.

Considerable progress occurred when it was realized that the ν_6 secular resonance (Wetherill and Williams, 1979; Scholl and Froeschlé, 1991) and 3:1 mean-motion resonance with Jupiter (Wisdom, 1985) are capable of directly pumping the orbital eccentricities of objects placed into them to Mars- and Earth-crossing values: since the velocity changes required to emplace fragments from neighbouring main-belt asteroids into these resonances is only ≃100 m/s, the process could be more efficient. In addition, the sparse data available on the orbits of chondrites pointed to an asteroidal source. In a series of papers (Wetherill, 1987, and references therein), this idea was extensively developed; analytical approximations for the resonant effects of the ν_6 and 3:1 resonances in combination with an Öpik–Arnold Monte Carlo orbital evolution model were used to conclude that the asteroid belt was capable of supplying the observed mass flux. We believe that the approximations involved in this approach produced a relatively unrealistic dynamical model, so that some inferences turn out to be incorrect.

The goal of this paper is to revisit the dynamics of transport of meteorites from the main resonances in the asteroid belt. We are primarily interested in discovering the dominant dynamical path followed by the majority of meteorites (the ordinary chondrites). We use direct numerical integrations that do not involve severe dynamical approximations. More specifically, we numerically compute the dynamical evolution of the orbits of thousands of test particles initially placed in the ν_6, 3:1 or 5:2 resonances, and we monitor their collision probability with the Earth. The comparison of the simulations with observed data allows us to draw some conclusions on the origin and dynamical history of chondrites.

The paper is structured as follows. "Numerical Simulations" discusses the simulation procedure. In "The Dynamical Evolution of Resonant Particles," we discuss the orbital evolution of particles initially placed in the ν_6, 3:1 or 5:2 resonances, independent of considerations of Earth impact. We then restrict ourselves to the case of the delivery of meteorites, giving in "Observed Quantities Related to Meteorite Dynamics" a brief review of the data available for a comparison with our simulations: these concern the orbital and radiant distribution of fireballs, the P.M./A.M. statistics of meteorite falls, and the cosmic-ray exposure (CRE) ages of meteorites. "Geometry and Probability of Earth Collision" discusses the important influence of the orbital geometry on both the collision probability with Earth and the atmospheric entry velocity. The orbital geometry also determines the probability of impact in the A.M. or P.M. hemisphere. In "Comparison with Recoverable Fireball Data," we simulate the orbital distribution of meteorites coming from ν_6, 3:1 or 5:2 resonances in a steady-state injection scenario taking into account different catastrophic collisional lifetimes. We compare these results with those coming from the fireball camera networks. In "Comparison with Meteorite Data," we turn our attention to the meteorite data, specifically the P.M. fall ratio and cosmic-ray exposure ages. Moreover, we simulate also the orbital distribution of meteorites coming from large single injection events occurring in the past, like those invoked to explain peaks observed in the meteorite CRE age distribution. In "Discussions and Conclusions," we discuss several scenarios on the origin of chondrites that are consistent both with the dynamical simulations and with the observational data. We also briefly discuss achondritic and iron meteorites.

NUMERICAL SIMULATIONS

Some of this work is part of a large collaborative project named GAPTEC (Gladman *et al.*, 1997), which attempted to determine if dynamical links could be established between asteroid families in the main belt and near-Earth asteroids (NEAs) of known taxonomic type; the GAPTEC acronym stands for Give a Parent to Each Child. This project integrated large numbers of particles placed in or near resonances in the main asteroid belt to observe the generic dynamical evolution and fates over a 100 Ma time scale. Details on the initial conditions are given in the next section.

The numerical integrations were accomplished using the "swift_rmvs3" integrator, designed by Levison and Duncan (1994). This code is based on the symplectic algorithm proposed by Wisdom and Holman (1991), which has been modified in order to handle planetary close encounters. Although the modified algorithm is not symplectic, the integrator handles the commonly occurring highly eccentric orbits very efficiently and, thus, the order of magnitude in speed gained makes it preferable to all other integration algorithms known to us. Discussions on the statistical accuracy of the swift_rmvs3 integrator can be found in Michel and Valsecchi (1996), Duncan and Lissauer (1997), and Dones *et al.* (1997). We include the direct gravitational effects on the meteoroids of all the planets from Venus to Neptune; this allows the inclusion of all important resonant phenomena on the small bodies.

In order to study the meteorite delivery process, we need to know not only the dynamical evolution of the test particles but also the evolution of their collision probability with our planet. Because the collision of a particle with the Earth is a rare event (<1% of the simulated particles strike a planet), it is not enough to record the collisions that we observe in our simulations. In order to improve our statistics, we have used a procedure developed in Wetherill (1967), which is an extension of the Öpik collision probability formulae to the case of two eccentric orbits. It is important to realize that the orbital histories have not been propagated using the Öpik–Arnold Monte Carlo method (Arnold, 1965). More precisely, our numerical simulations provide a time history of the orbital elements a, e, and i for each particle. For every set (a, e, i), the collision probability with the Earth and the average impact velocity are computed averaging over all possible orbital configurations occurring during a precessional cycle of the orbits and taking into account the Earth's gravitational focusing. This procedure has been accomplished with a numerical code implemented by Farinella and Davis (1992) and kindly provided to us. Although resonant protection mechanisms can in principle invalidate the results, Milani *et al.* (1989) have shown this procedure to be statistically accurate within a factor of 2. As an additional test, we have applied this procedure to numerical simulations of the evolution of lunar and Martian ejecta (Gladman *et al.*, 1996), examining Venusian and Earth impacts, respectively, where up to 30 collisions were recorded, and we have compared the computed

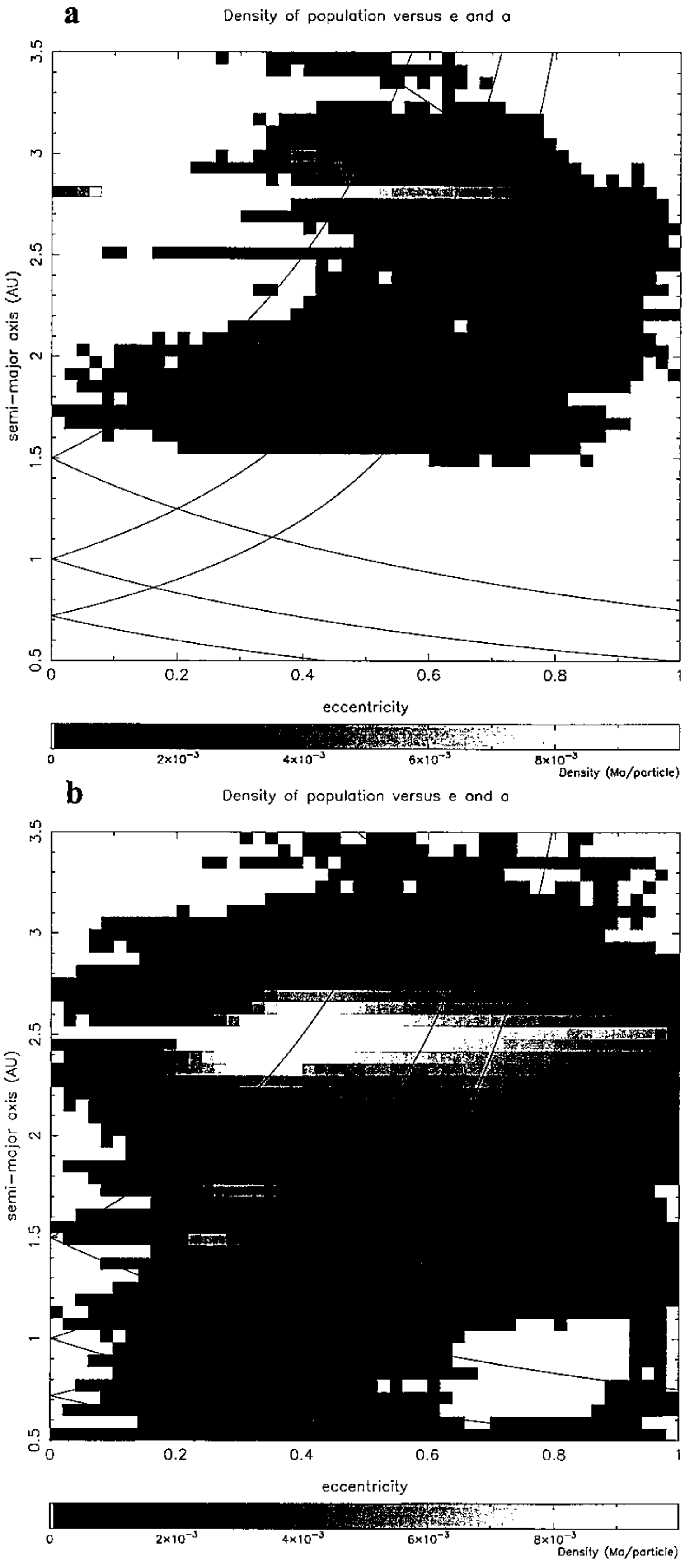

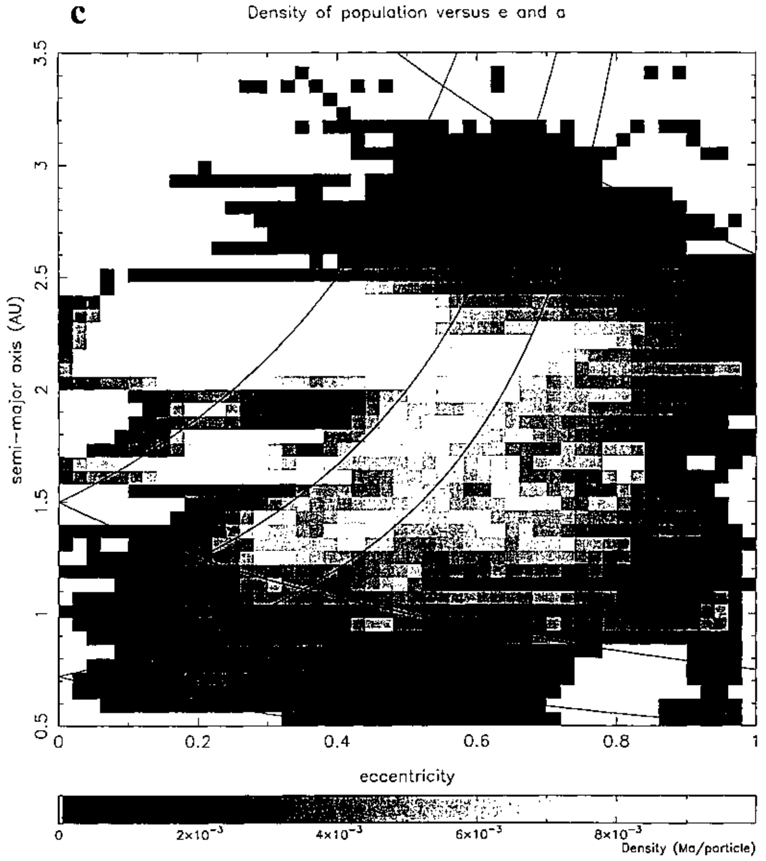

FIG. 1. (left and above) Residence times on the e, a plane for a set of particles coming out of the 5:2 (plot a), 3:1 (plot b) and ν_6 resonances (plot c). The total time spent in each cell of the e, a plane has been normalized by the number of active particles, so that the grey-scale gives the average duration of residence per particle or, equivalently, the expected density of meteoroids in a scenario of steady-state injection into resonance (if an infinite collisional lifetime is assumed).

cumulative collision probability with that observed in the simulation. The results agree within a very satisfactory factor of 30%. Curiously, the collision probability provided by Öpik's method always underestimates in our tests the real collision rate. Wetherill and Chambers (1997) obtained collision results very similar to ours for the 3:1 resonance using a different numerical approach.

THE DYNAMICAL EVOLUTION OF RESONANT PARTICLES

Initial Conditions

As discussed in Gladman *et al.* (1997), outer-belt resonances are very inefficient sources of long-lived Earth-crossing particles because the proximity of Jupiter will result in their rapid removal; particles at high eccentricities are protected from Jovian close encounters by mean-motion resonances, but an encounter with an inner planet can suffice to remove this protection, after which they are removed from the system in $<10^5$ years. Thus, we confine our attention to the ν_6 secular resonance, and the 3:1 and 5:2 mean-motion resonances. The GAPTEC project conducted 100 Ma integrations of the orbital evolutions of 382 fictitious particles in the 5:2 resonance, 393 in the 3:1 resonance, and 110 in the ν_6 resonance. Consistent with the purposes of the project, the initial conditions of the particles were chosen in order to simulate bodies injected into the resonances from the closest asteroid families (Gladman *et al.*, 1997; Morbidelli *et al.*, 1996).

These initial conditions sample the 5:2 and 3:1 resonances at three eccentricity/inclination regions with no specific selection towards the most unstable portions of such resonances. Some particles were placed close to the resonant borders in order to study possible phenomena of late capture into resonance due to slow chaotic diffusion. The number of particles reported above, and our statistics below, are based on the "active" particles, namely those that ever interact with the resonance (showing librations of the critical resonant angle) during the integration timespan; actually 480 particles were integrated in/close to each resonance. We find that for active particles, the fates in these two mean-motion resonances are basically independent of the starting location (see Gladman *et al.*, 1997). Therefore, the simulations are suitable to investigate the typical dynamical evolution of meteoroids injected anywhere in these resonances. Nevertheless, in order to have better statistics on the evolution of particles from the important 3:1 resonance, we integrated 987 additional particles for 50 Ma, initially uniformly distributed in the resonance having inclinations of 10° and eccentricities ranging from 0 to 0.3; the evolution was statistically identical to that of particles studied in the framework of the GAPTEC project.

The case of the ν_6 resonance is different, because the 110 particles studied in the GAPTEC project were all emplaced in the strongest part of the resonance, where ejecta coming from the asteroid 4 Vesta might arrive (see Migliorini *et al.*, 1997). To remedy the induced time scale bias, we integrated an additional 300 particles for 50 Ma, sampling the resonance at different inclinations and uniformly covering not only the rapidly unstable portions of the ν_6 resonance, where the eccentricity is directly pumped to Earth-crossing values, but also the parts where the eccentricity is pumped to more limited values (Mars-crossing or less). For this integration, only test particles that had at least one close encounter with a planet during the integration timespan have been considered "active" (193 of the 300).

General Results

The dynamical evolution of particles initially located in the main resonances in the asteroid belt has been discussed already in Gladman *et al.* (1997). Here we recall the basic features that should be kept in mind in order to understand the meteorite delivery process.

The central parts of the ν_6 resonance, and the 3:1 and 5:2 mean-motion resonances are very efficient in pumping the eccentricities of resonant bodies. In contrast to previous discussions (Wetherill and Chapman, 1988; Greenberg and Nolan, 1989), these resonances tend to pump the eccentricity not just to moderate planet-crossing values of 0.3–0.6 but all the way to $e \sim 1$ on a typical time scale of 1 Ma. If the eccentricity becomes nearly unity, the perihelion distance decreases below the solar radius, and the resonant particle collides with the Sun (Farinella *et al.*, 1994). This is a dramatic change of emphasis: only the particles that are extracted from the resonances by the inner planets could live, in principle, significantly longer than 1 Ma. By "extraction," we mean a close encounter that moves the semimajor axis (or possibly e and i for the ν_6 resonance) enough to take the particle out of the resonance.

Mars is able to extract only a few percent of resonant bodies before Earth-crossing is achieved. There has been discussion in the literature (see Greenberg and Nolan, 1989, and references therein) that such particles could then be transported by Martian encounters to the Earth following a very slow path (time scale 100 Ma–1 Ga), but actually the "kicks" provided by Martian encounters are so small that the particles cannot jump over the resonances and (after a typical time ranging from one to a few tens of million years) always find themselves again injected into some resonant mechanism that pumps them to Earth-crossing orbits. Of all of our integrated particles, none ever reached an Earth-crossing orbit following this conjectured Martian slow track.

The Earth and Venus are much more efficient than Mars in extracting bodies from resonances. It was expected (see Bottke *et al.*, 1996) that such particles evolved under the effects of planetary close encounters along a line of quasi-constant Jacobi value (the Jacobi constant would be exactly conserved in the circular restricted three-body problem). In reality the dynamics are very much more complicated: there are many high-order resonances that force the orbits to evolve transversally with respect to constant Jacobi lines (see Michel *et al.*, 1996), so that the Jacobi constant is very poorly conserved on a million year or longer time scale and, in practice, extracted particles are quickly spread all over the Earth- and Venus-crossing region. The "mortality" of the extracted particles is still very high. Those that are driven by close encounters to $a > 2.5$ AU are usually ejected by Jupiter on hyperbolic orbits. Many others are injected again into the 5:2, 3:1 or ν_6 resonances and subsequently are forced to collide with the Sun.

As a result of all these mechanisms, the median lifetime of our simulated particles (ν_6, 3:1 and 5:2 resonances) is in the range 2–3 Ma, and only ~10% of them survive for $\simeq$10 Ma (see Fig. 2 of Gladman *et al.*, 1997). In order to live much longer than the median lifetime, objects must reach semimajor axes <1.8 AU. We will hereafter call orbits with $a < 1.8$ AU evolved orbits. In this region, although many resonances exist and influence the dynamics (Michel and Froeschlé, 1997; Michel, 1997), no statistically significant dynamical mechanisms have been found that pump the eccentricities up to Sun-grazing values. Therefore, evolved particles die only by colliding with a planet (rare) or after being driven back to $a > 1.8$ AU (after a typical 1–10 Ma journey) and then usually being pushed by a resonance into the Sun.

We now proceed to discuss in more detail the dynamical evolution of particles placed in the 5:2, 3:1 and ν_6 resonances. To illustrate where the particles go, and how long they stay there, we have divided the (e, a) plane into cells of width 0.02 × 0.06 AU and have computed the total time spent in each cell. Figure 1a–c shows the result of the computation in grey-scale plots; the residence time has been normalized by the number of active particles (so that the three plots can be compared directly) and shows the amount of time an "average" particle injected in the corresponding resonance spends in various regions of the orbital elements space.

The 5:2 Resonance

The 5:2 resonance is the one that pumps orbital eccentricities on the shortest time scale. Since it is located at $a = 2.8$ AU, ~90% of the particles, once at large e, come under the control of Jupiter and are ejected on hyperbolic orbits. Very few particles evolve to smaller semimajor axis under Earth and Venus encounters (Fig. 1a); only 5 out of our 382 reached the evolved status ($a < 2$ AU). The median lifetime of the particles originally in the 5:2 resonance is only about one-half million years, although just 10% of them survive more than 3 Ma.

The 5:2 resonance exhibits an interesting phenomenon, first observed by Milani and Farinella (1995): particles initially outside the resonance, but very close to its border (0.001 AU), can slowly leak in and be captured by the resonance after several million years due to slow chaotic diffusion. Once captured, these particles evolve on short (<1 Ma) time scales like those initially placed inside the resonance. This phenomenon is important in principle because it permits an increase of the dynamical lifetime of a small fraction of particles to tens of million years, thus producing a long-lived "tail" in the lifetime distribution. However, because only a small fraction of particles would be expected to be in this tiny strip bordering the resonance, it is unlikely that this pheonemenon dominates the meteorite delivery process.

The 3:1 Resonance

The 3:1 resonance is located at 2.5 AU. Wisdom (1985) showed that the resonance pushes all particles to Mars-crossing, and some to Earth-crossing orbits; later work (see Moons, 1997 for a review) showed that the resonance can pump particle eccentricities nearly to unity. Even at $e \simeq 1$, particles in the resonance do not quite cross the orbit of Jupiter; and in any case, the resonance protects them from Jovian close encounters. Therefore, only particles that are extracted and pushed to larger semimajor axis (27%) are taken under the control of Jupiter and ejected. All the others (except for a few percent that suffer collisions with terrestrial planets) die colliding with the Sun; 28% of the particles do so without ever leaving the resonance, whereas the remainder are first temporarily extracted by the Earth or Venus. The median lifetime of the particles is of the order of 2 Ma, although only 10% of them survive more than 7 Ma. Figure 1b shows the spread of the particles on the (e, a) plane. The resonance at 2.5 AU is obvious in this figure. Note that much more time is spent in the evolved state than in the 5:2 case but that the particles still mostly reside in the vicinity of the resonance.

The ν_6 Resonance

This resonance occurs when the longitude of perihelion of the small body precesses at the same rate as the sixth secular frequency of the planetary system (~28.2 arcsec/year, which is also the averaged precession rate of Saturn's perihelion). The exact center of this resonance (the dark curve in Fig. 2) depends on the orbital inclination, but only weakly on the eccentricity (Morbidelli and Henrard, 1991), and is known to bound the inner edge of the main asteroid belt (Froeschlé and Scholl, 1989); the powerful 4:1 mean-motion resonance (at $a \simeq 2.06$ AU) is also nearby (Beust and Morbidelli, 1996).

In contrast to the 5:2 and 3:1 mean-motion resonances, the ν_6 secular resonance (neglecting the presence of the inner planets) has a less chaotic structure (Morbidelli, 1993). The ν_6 resonance forces periodic oscillations in the eccentricity of particles placed near it on a time scale of $\simeq$1 Ma. Close to its center, the resonance forces particles to cross the orbit of the Earth (or Venus) or even collide with the Sun during the highest eccentricity portion of their cycle; we call this the "powerful" portion of the resonance. Further from the center, the value of the maximal eccentricity sharply drops, so that only Mars-crossing is achieved on a portion of the cycle; in order to become Earth-crossers, particles in this border region must slowly evolve, under the effect of solely Martian close encounters, until they reach by chance the central part of the resonance. In fact, the resonance does not have a sharp "edge" in the sense of the other resonances; but for our purposes, being unable to reach Mars provides a useful definition for being "inactive." For a detailed description of the very complicated structure of the ν_6 resonance, see Morbidelli (1993).

Figure 2 shows the time scales of these processes. The six boxes display the results of six numerical experiments concerning particles with initial inclinations equal to 2.5, 5, 7.5, 10, 12.5, and 15°, all with $e = 0.1$. The angle $\varpi - \varpi_S$, the difference between the perihelion longitudes of the particle and that of Saturn, was initially set to zero. In each experiment, initial semimajor axes were evenly spaced on a grid with a resolution of 0.003 AU. The dots denote the time required to become Earth-crossing as a function of the initial semimajor axis. As anticipated above, deep inside the resonance particles become Earth-crossers in <1 Ma; whereas, further from the center of the resonance, the time required increases sharply. The upper limit of 50 Ma is imposed by the length of the integration. The particles at the right edge of each box (crosses) never encountered Mars, so that we expect that they would never reach the center of the resonance and become Earth-crossers. On the basis of this simulation, we can conclude that the ν_6 resonance has a region of width 0.03–0.06 AU (depending on the inclination) where particles become Earth-crossers only on time scales of tens of million years. This mechanism has been discussed by Wetherill (1974), but here the quantitative extent of the border region and time scale has been provided. Note that, although this time scale is long compared to the "fast-track" ones discussed above, it is shorter than the ~10^8 years conjectured previously (Wetherill, 1987).

Once in the powerful portion of the resonance, particles are characteristically eliminated in a few million years. About 80% of the particles die impacting the Sun, whereas very few particles (12%) are pushed to $a > 2.5$ AU and are eliminated by Jupiter

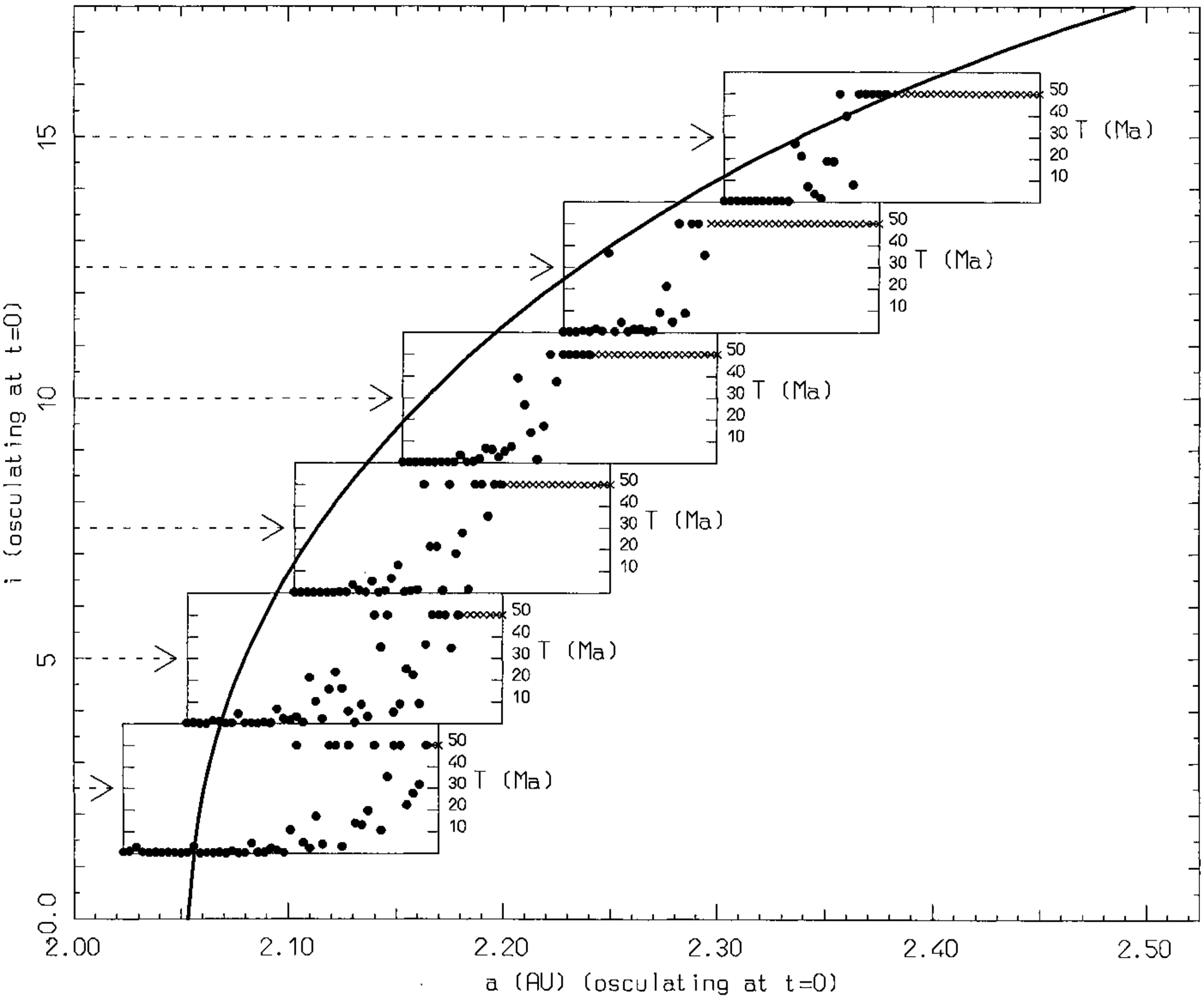

FIG. 2. The time required for particles placed in or near the ν_6 resonance in the main belt to reach Earth-crossing orbits. The figure shows the results of six numerical simulations at different inclinations (from $i = 2.5°$ to $i = 15°$ with 2.5° intervals) covering 50 Ma. For each of the considered inclinations, the arrow points to a panel showing the time required to reach $q = 1$ AU as a function of the initial a. Dots refer to test particles that suffer encounters with Mars, whereas crosses refer to particles that never have encounters with Mars so that they are expected to be stable and never be able to enter deeper into the resonance. A change in the intial phase of the resonant angle $\varpi - \varpi_S$ can slightly modify the semimajor axis dependence of the results at each inclination. The solid line shows the center of the ν_6 resonance at $e = 0.1$. See the text for further discussion.

(Fig. 1c). The median lifetime is ~2 Ma, whereas the time required to reduce the population to 10% of the original is ~20 Ma. The latter time scale is much longer than in the 5:2 and 3:1 resonances because the ν_6 is by far the resonance that produces the largest number of evolved orbits. The evolved particles survive in that state for long enough that the residence times (Fig. 1c) for $a = 0.5–2$ AU have noticably increased with respect to Fig. 1a,b. These evolved particles die predominantly by having their semimajor axes raised again to $a > 2$ AU and impacting the Sun.

OBSERVED QUANTITIES RELATED TO METEORITE DYNAMICS

Direct observation of the orbital distribution of submeter bodies in space is not feasible and, thus, the only orbital information we have for meteorite-sized bodies is supplied by those objects that hit the Earth's atmosphere. To increase the available orbital data, automatic camera surveys (Ceplecha, 1977; Halliday *et al.*, 1978; McCrosky *et al.*, 1978) were conducted to compute from the observed fireball trails the orbital distribution of the incoming particles that create them. The camera network projects have succeeded in establishing that chondrites come from an asteroidal, and not cometary, source, but many of the observed fireballs likely involved cometary material. Wetherill and ReVelle (1981) selected, among fireball events observed during the Prairie Network campaign, those that should correspond to ground-recoverable meteorites of chondritic composition. A selection based on dynamically determined terminal masses was performed by Halliday *et al.* (1996) on the data from the Canadian MORP campaign, which led to qualitatively similar results. We have combined the results published in both of these papers to form a database consisting of orbital elements, entry velocities, and radiant directions.

Figure 3 presents the orbital elements distribution. The concentration towards having $q = 1$ AU (Fig. 3c) is enhanced by the larger Earth-collision probability of particles on such orbits (see the following section), and, thus, the orbital distribution in Fig. 3 is not the same as the true distribution of meteoroids in space. We find below that the semimajor axis distribution is a more useful discriminant of source resonance than the perihelion distribution and, thus, confine our attention to the latter for the remainder of our discussion. We remark that the number of particles *vs.* semimajor axis has a generally increasing trend from 0.6 to 2.5 AU, which indicates that the current contribution from evolved orbits is smaller than those from objects still near the main belt (only ~40% of the fireballs have $a < 1.8$ AU). The fact that dynamical mortality in the region $a > 2$ AU is so efficient implies that this region must be continuously repopulated, at least during the last few million years. Also shown in Fig. 3a (as large circles) are the data for the Peekskill H6 ($a = 1.49$, $e = 0.41$, $i = 4.9°$, Brown *et al.*, 1994), Innisfree LL ($a = 1.87$, $e = 0.47$, $i = 12°$, Halliday, 1978), Pribram H5 ($a = 2.40$, $e = 0.67$, $i = 10.5°$) and Lost City H5 chondrites ($a = 1.67$, $e = 0.42$, $i = 12°$) (both in Wetherill and ReVelle, 1981). As the only four photographically recorded recovered fireballs, they are especially interesting, but it should be noted that they are also exceptionally large by fireball standards.

The preatmospheric velocity, or entry velocity, of the selected fireballs from Wetherill and Revelle (1981) and Halliday *et al.* (1996) are plotted below (Fig. 8) when we compare them with the results of our simulations. The angular deviation α of the apparent radiant of the fireball with respect to the antiapex of the Earth's velocity vector is a second well-determined observational quantity related to the orbital distribution (see the following section) and will also be plotted (Fig. 9d) below. The inclination distribution of fireballs is also shown in Fig. 9b.

This fireball orbital data must be considered our best approximation of the prefall orbital distribution of Earth-encountering chondrites. However, although the preatmospheric sizes of the particles associated with the fireball data range from 1–10 cm (Wetherill and Revelle, 1981), the typical preatmospheric size of ground-recovered meteorites is tens of centimeters (Bhandari *et al.*, 1980), due to evident recovery biases. This implies that the median collisional lifetime of recovered meteorites and of fireball-producing particles should be different, so that the orbital distribution of meteoroids producing typical falls could be different from that shown in Fig. 3.

Except for the four photographically observed meteorites discussed above, little direct orbital information is available for recovered meteorites. The most important available statistic is the meteorite's time of fall. As discussed in the following section, the ratio between the number of afternoon falls over the total number of falls (the P.M. ratio) is an indicator of the typical perihelion distance of meteorite orbits (see also Wetherill, 1974 and Greenberg and Nolan, 1989). Ordinary chondrites generally have P.M. ratios of ~68% (Graf and Marti, 1995) but show differences among the various mineralogical types (*e.g.*, H5 chondrites have a P.M. ratio of only 48%). Unfortunately, one cannot be sure that the observed P.M. abundance is not systematically biased towards a higher P.M. ratio; even though many chondrite falls are observed by farmers working in fields (Wetherill, 1968), one is concerned that most people spend more time outside in the afternoon than in the morning so that the period between 12:00 A.M. and 6:00 A.M. is underrepresented (Wetherill, 1987). To partially correct this bias, the P.M. ratio is calculated usually based only on falls between 6:00 A.M. and 6:00 P.M. Note that even if such a systematic bias exists, it cannot depend on chondrite type, and thus the relatively lower P.M. ratio for the H5 chondrites is still real. There also exists some observations (discussed in Wetherill and ReVelle, 1981) of the radiant distribution of falls; because the determination of apparent radiants by unskilled observers is difficult, we will not consider this data set, especially in light of the fact that the camera network radiants are vastly better determined.

Another important constraint for meteorites is their cosmic-ray exposure (CRE) age. The CRE age of a meteorite measures the time interval in space between the meteoroid's formation as a body of <3 m diameter (following removal from a shielded location within a larger object) and its arrival at the Earth. Figure 4 shows the number of meteorites *vs.* exposure age for L, LL, and H chondrites, in semi-logarithmic scale. The average/median exposure ages of the plotted L, LL, and H chondrites are 22/19, 20/15, and 14/8 Ma, respectively. The exceptionally prominent ≈8 Ma peak in the H-chondrite distribution, which is generally agreed to represent a recent large event, although Graf and Marti (1995) discuss the possibility that two events are present, unrepresentatively skews the average transfer age for that class. It should be noted, moreover, that many of the low exposure age (<4 Ma) chondrites have evidence for complex exposure histories, which means their actual transfer times were longer by up to an order of magnitude (Graf and Marti, 1995; Herzog *et al.*, 1997). Recall that complex exposure histories result when the CRE geometry changes, such as during a collisional event that alters the size of the body containing the meteorite.

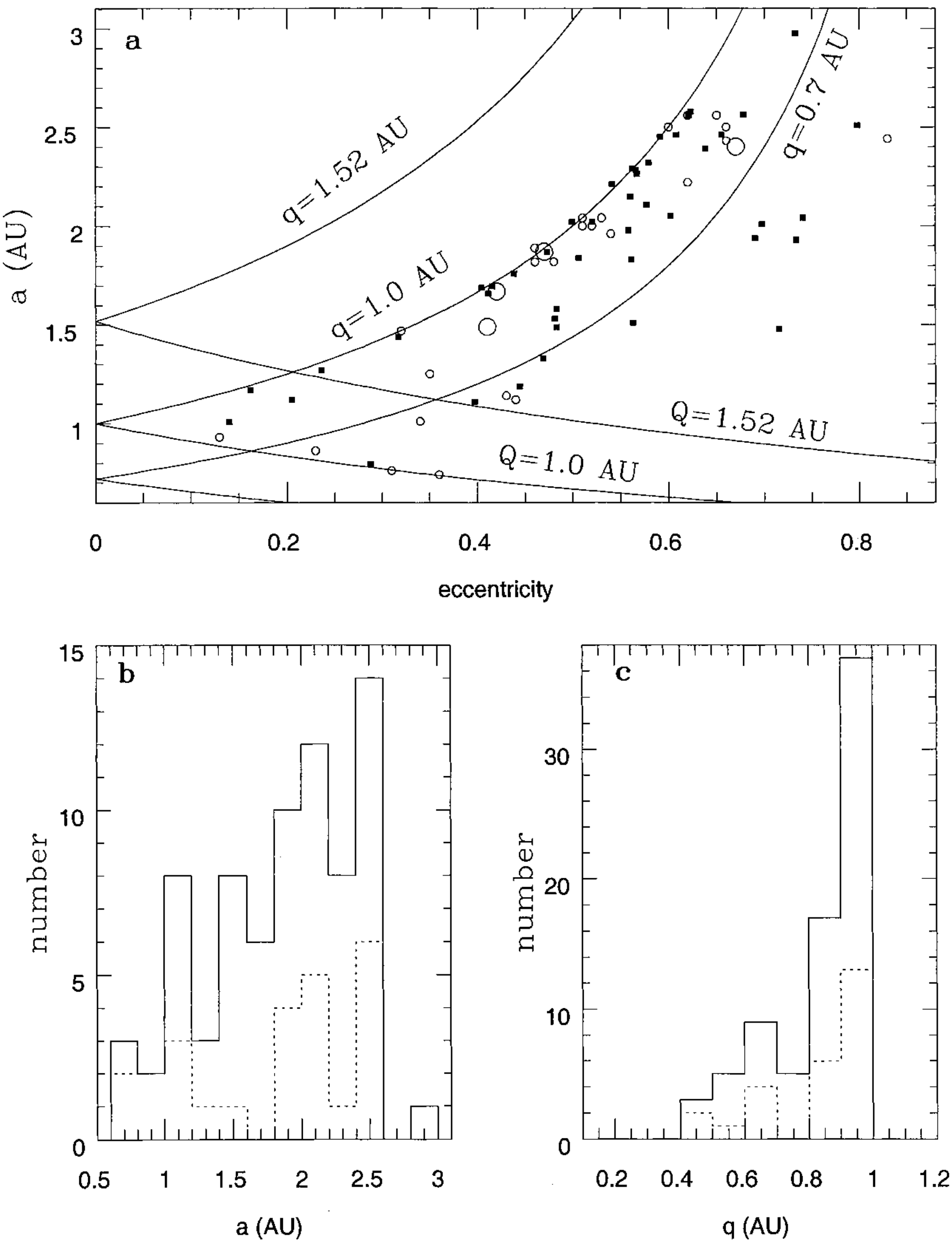

FIG. 3. (a) The orbital distribution (inclinations not shown) of the observed fireballs thought to be chondritic objects capable of dropping meteorites. Open circles indicate Wetherill and Revelle (1981) data, solid squares indicate Halliday *et al.* (1996) data. Large open circles indicate the four recovered, photographically observed fireballs. (b) The binned semimajor axis distribution of these objects. (c) The binned perihelion distribution of these objects. In (b) and (c), the dotted (lower) histogram indicates just the Wetherill and Revelle subset.

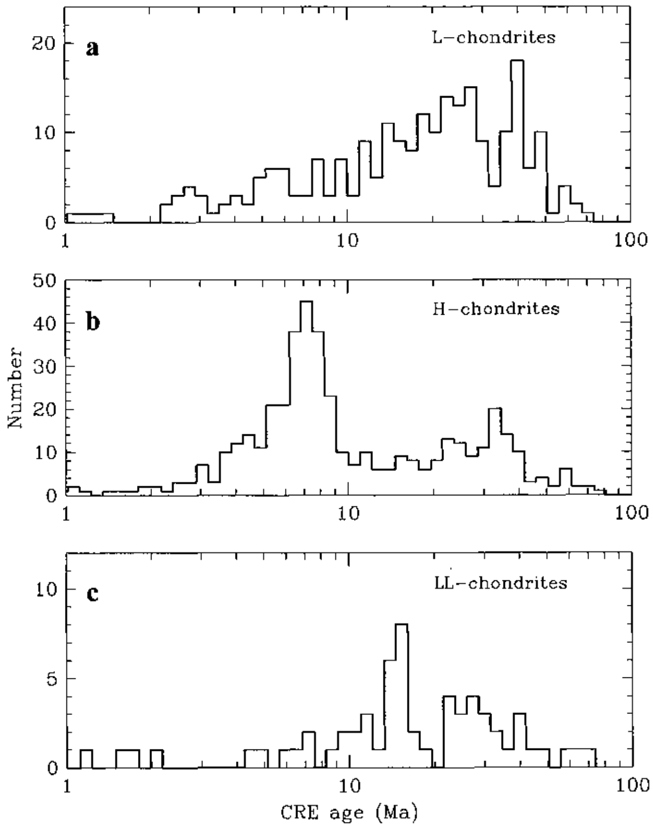

FIG. 4. The number of meteorites *vs.* cosmic-ray exposure age for H, L and LL chondrites, from data kindly provided to us by T. Graf (pers. comm.). For the H and LL chondrites, we include Antarctic meteorites, which causes some slight excess clumping due to multiple falls, but a comparison with Marti and Graf (1992) shows that this is a minor qualitative effect.

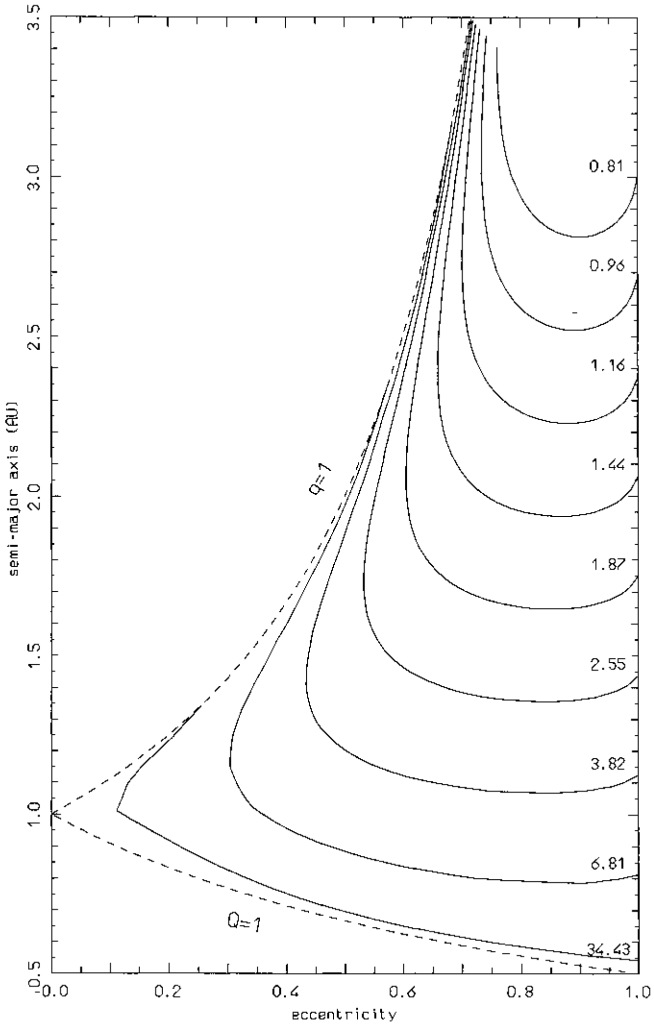

FIG. 5. Collision probability per unit time with Earth as a function of orbital geometery, for $i = 1°$ orbits. The unit is 10^{-8}/year and, thus, a probability of 1 on this plot corresponds to a lifetime of ~100 Ma with respect to Earth collisions; of course because the particles have a dynamical lifetime much shorter than 100 Ma, only a small fraction of them can strike the Earth. The dashed curves denote the set of orbits with $q = 1$ AU or $Q = 1$ AU (q and Q being the perihelion and aphelion distance, respectively) and, thus, delimit Earth-crossing space.

The CRE histograms generically show a somewhat bell-shaped distribution with superimposed peaks, although the statistical relevance of specific peaks is a continual subject of debate. The underlying bell shape (especially obvious for the L chondrites) is usually interpreted as the result of a steady-state flux of meteorites to the Earth convolved with an exponential decay in time of the number of meteorites due to a finite collisional or dynamical half-life (Marti and Graf, 1992; Welten *et al.*, 1997). This is of course a simplified interpretation that does not take into account any specific feature of the dynamical process of transport of meteoroids from the asteroid belt to an Earth-colliding orbit. A major contribution of our paper is to provide the dynamics explicitly, thus decoupling the collisional and dynamical effects.

The orbital distribution of fireballs, the P.M. fall ratio of meteorites, and the distribution of their exposure ages are the observational constraints that, in conjunction with our dynamical model, will allow us to design scenarios about the meteorite delivery process. However, we must first establish the link between the dynamical histories of particles leaving the belt and the expected flux at the Earth.

GEOMETRY AND PROBABILITY OF EARTH COLLISION

As explained at the end of "Numerical Simulations," for every a, e, i, characterizing an orbit, we can compute the averaged collision probability P with the Earth by numerically averaging over the possible orbital orientations. Figure 5 shows the collision probability per unit time on the e, a plane for $i = 1°$. Away from $q = 1$ and $Q = 1$, the collision probability modestly increases with decreasing semimajor axis mostly because the orbital period of the particle decreases. The sharply increased probability near $q = 1$ and $Q = 1$ is due to the increased likelihood of encountering the Earth when the meteoroid's orbit is tangent to that of the Earth's (Öpik, 1976). Therefore the evolved orbits, which are the longest living ones, are those that tend to have the highest Earth-collision probability. As a consequence, the rarer meteoroids on evolved orbits contribute a disproportionately large number of deliveries. The collision probability drops by one order of magnitude when passing from 1° to 15° and by another factor of 2 from 15° to 30°.

The position in e, a, i, space also determines the impact geometry with our planet and the probability to fall in the afternoon (noon–midnight) or in the morning hemisphere. For example, meteorites on orbits with aphelion $Q = 1$ encounter the Earth at their aphelion, while they are moving parallel to the Earth's motion but with slower speed, and thus fall on the Earth's leading hemisphere if one neglects graviational focusing and obliquity of the Earth's spin axis (both discussed below). In other words, the local time at the place of fall is between midnight and noon so that all falls are A.M. falls. The apparent unfocussed radiant direction will have an angle $\alpha = 180°$ with the antiapex direction of the Earth's motion. Conversely, meteoroids on orbits with $q = 1$ catch the Earth from behind, and thus the local time at the place of fall is between noon and midnight so that all are P.M. falls, and $\alpha = 0$ for unfocussed radiants. Neglecting gravitatational focusing and the Earth's obliquity, one can compute for each point of the a, e, i, space the probability to impact the Earth on the afternoon hemisphere (Valsecchi and Manara, 1997). The result is shown with level curves in Fig. 6 for the $i = 0$ case. In the region $a > 1$ AU, the P.M. ratio depends basically on the perihelion distance.

Two effects alter the P.M. ratio from that shown in Fig. 6. Gravitational focusing reduces extremely high P.M. or A.M. fall probabilities (because of symmetry, it has no effect when the P.M. ratio is 0.5) but is effective only for meteoroids encountering Earth with relative velocities less than Earth's escape velocity of 11.2 km/s, or equivalently with velocities at the top of the atmosphere $v_a <$ 16 km/s. The Earth's obliquity also causes a convergence towards a 50% P.M. ratio due to the fact that there is no longer a correspondence between the leading/trailing hemisphere and the A.M./P.M. hemisphere. We directly include these effects in our calculations of the P.M. ratio by randomly choosing impact parameters and day of encounter for the incoming meteoroid and then calculating the impact point relative to the solar longitude on the Earth. To illustrate for coplanar orbits with $a = 2.5$ AU and $e = 0.61$, 0.70, 0.77, and 0.90, the P.M. ratios change from 91%, 61%, 50%, and 36% to 80%, 59%, 50%, and 37%, respectively, when focusing and the obliquity are taken into account. Therefore, Fig. 6 is intended as a qualitative guide; for quantitative comparisons between our simulations and the observations, we have always included these two effects.

For meteorite-sized bodies, those entering the atmosphere at higher speeds suffer greater ablative mass losses (ReVelle, 1979); this ablation may produce a terminal mass so small that no recoverable object results. The entry velocity depends on the orbital elements of the impactor's orbit. In Fig. 6, the three bold curves denote, still in the $i = 0$ case, entry velocities equal to 16 km/s, 20 km/s and 31 km/s. Note that the entry velocity is not simply the relative velocity between the Earth's and the impactor's orbit but is increased by the Earth's gravitational acceleration; thus, entry velocities lower than the Earth's escape velocity of 11.2 km/s are impossible. Most recoverable meteorites have entry velocities <20–23 km/s (Wetherill and ReVelle, 1981). Eighty percent of the fireballs in the sample shown in Fig. 3 have entry velocities <20 km/s, which is a velocity used by Wetherill and Chambers (1997) as a cutoff. For reasons discussed in the following section, we prefer to use a more relaxed cutoff of 31 km/s. As shown in Fig. 6, the entry-velocity bias causes meteorites on orbits with $a > 2$ AU to fall preferentially in the afternoon hemisphere, and decreasing the entry-velocity cutoff increases the P.M. ratio. Only evolved orbits populate regions where A.M. fall excesses occur. Figure 6 depends strongly on the inclination; for larger inclinations, the $q = 1$ curve no longer exhibits an unfocussed 100% P.M. ratio, and the region of the a, e plane associated with an excess of A.M. falls increases. The entry-velocity level curves move towards smaller eccentricities as inclinations increase, and, for example, at $i = 25°$ the 20 km/s curve intersects the $q = 1$ AU curve at $a = 2$ AU.

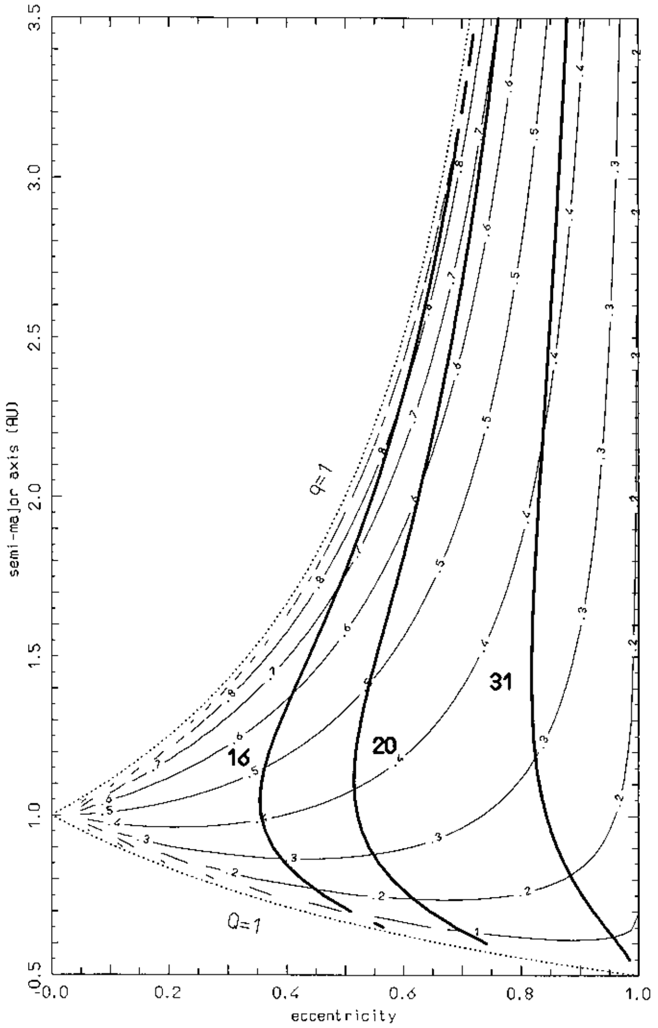

FIG. 6. P.M. ratios of meteorite falls and atmospheric entry velocity v_a as a function of orbital geometry for $i = 0°$. The bold curves give contours of constant v_a in km/s. The dotted curves denote the set of orbits with $q = 1$ AU or $Q = 1$ AU. The light curves denote the fraction of P.M. falls from that orbit. Gravitational focussing and Earth's obliquity (see text) have been neglected.

A final physical effect that must be considered is the importance of collisions in both the production and destruction of meteoroids in space. The catastrophic collisional half-life (defined as the time scale for the meteoroid to suffer an impact leaving a fragment less than half the original mass) of meteoroids that are crossing the main asteroid belt is estimated to be on the order of

$$\tau \approx 1.4\sqrt{r_{cm}}\ \text{Ma} \qquad \text{Eq. (1)}$$

where r_{cm} is the meteoroid radius in centimeters (see Wetherill, 1985; Farinella *et al.*, 1997). Bottke *et al.* (1994) calculate that the collisional lifetime rises by one to two orders of magnitude after the particle orbit decouples from the asteroid belt (*i.e.*, it has $Q <$ 1.8 AU). The disruption of a body larger than several meters in radius presumably liberates large numbers of fragments that are then small enough to accumulate CRE. Fireballs of 1–8 cm in radii (Wetherill and ReVelle, 1981) have collisional lifetimes of ~1–3 Ma; whereas, the preatmospheric mass range of 1–1000 kg (8–80 cm) for meteorites (Bhandari *et al.*, 1980) implies a collisional lifetime range of ~3–10 Ma.

COMPARISON WITH RECOVERABLE FIREBALL DATA

For each of our available simulated evolutionary histories, we have computed the Earth-collision probability, the atmospheric entry velocity, and the radiant distribution at each output epoch. The ν_6 results are based on the GAPTEC Vesta family simulation (Gladman *et al.*, 1997; Migliorini *et al.*, 1997) of 110 particles and the 193 active particles of the new ν_6 simulations reported in Fig. 2. The 3:1 results are the compilation of the three GAPTEC simulations in the 3:1 resonance (containing 92, 145, and 156 active particles) with the 987-particle simulation. The 5:2 results are based on the three GAPTEC simulations of that resonance. In order to compare the results of the simulations with the data, we must estimate a collisional lifetime and a velocity bias. We do this systematically by examining the semimajor axis distribution to determine the collisional effects and the entry-velocity distribution to determine the velocity bias because these two distributions are the most sensitive to those two effects.

Semimajor Axis Distribution

The left column of Fig.7 shows the probability of impacting the Earth as a function of the orbital semimajor axis for particles coming out of the ν_6, 3:1, and 5:2 resonances, integrated over the entire orbital history of all particles and normalized by the number of particles. Thus, each bin reports the fraction of meteoroids from that resonance that arrive at the top of the Earth's atmosphere. These histograms can be considered to be the semimajor axis distribution of incoming meteorites in a scenario of steady-state injection into resonance. No velocity bias has been imposed on this figure (although we will include this below).

The light (upper) histograms correspond to no collision effects being important. For the ν_6 particles, this shows a relatively flat distribution ranging from ~1 to 2 AU (Fig. 7a). This occurs because the higher collisional probability of evolved orbits (Fig. 5) compensates for the fact that only a fraction of the particles live for a significant time in the evolved state. The light histogram for the 3:1 resonance (Fig. 7b) shows a well-defined peak centered at 2.5 AU because the majority of the injected particles do not have time to disperse far from the resonance (Fig. 1b). The important contribution of particles on evolved orbits is clearly visible. Only the inefficient 5:2 resonance (Fig. 7c) shows no relevant meteorite-producing population on evolved orbits because none of our simulated particles reached semimajor axes <1.5 AU (see "The 5:2 Resonance"). Only gross features of these histograms should be taken as reliable, due to noise present from the limited number of integrated particles, which results in single particles occasionally reaching very high collision probability states. By plotting subsets of the data, we conclude that the following features are robust: (1) the "flat" distribution for the ν_6 in the range 1–2 AU, (2) the rarity of meteorites coming from above $a = 2$ AU for the ν_6 resonance, (3) the very strong peak at $a = 2.5$ AU for the 3:1 resonance, and (4) the presence of an important (but late-arriving, see below) evolved component from the 3:1 resonance. Introducing a velocity cutoff on this figure modifies none of these conclusions.

The semimajor axis distribution of chondritic fireballs (Fig. 3b) does not resemble any of the light histograms of Fig. 7a–c. The ν_6 resonance is too flat and lacks particles above $a = 2.2$ AU, the 3:1 resonance has too strong a peak at 2.5 AU and too many evolved particles, and the 5:2 resonance has its strongest feature near the resonance at 2.8 AU where no fireballs are present. The relative deficit of evolved fireball orbits in Fig. 3b indicates that a process is operating that prevents 1–10 cm radius particles from reaching evolved orbits. One expects this to be a collisional effect since the collisional half-life estimates (Eq. 1) of particles this size are on the order of or smaller than the time required to reach the evolved orbits. To incorporate this effect, at each timestep t we have multiplied the Earth-collision probability of each particle by its "probability to exist" $2^{-A/\tau}$. This is equivalent to saying that collisions produce a cascade that essentially reduces half of the original objects to unrecoverable meteoroids on the time scale τ. Here the "effective main-belt age" A is the cumulative time between 0 and t that the particle has spent on an orbit with $Q > 1.8$ AU (*i.e.*, coupled to the asteroid belt, cf. Rabinowitz, 1997). By varying the 1.8 AU inner edge, we find our results to be quite insensitive to this distance in the range 1.8–2.1 AU and remark that most particles spend only a small fraction of their lifetimes decoupled.

The shaded and black histograms in Fig. 7a–c correspond respectively to $\tau = 10$ Ma and 3 Ma half-lives. As expected, the introduction of a finite half-life due to collisions modifies the simulated orbital distribution of meteorites by reducing the relative contribution from those on evolved orbits. This is because the meteoroids on evolved orbits are the oldest ones because particles take several million years to evolve to small semimajor axes under the effect of Earth and Venus close encounters, so that collisional effects preferentially remove particles that eventually descend towards 1 AU (especially obvious in the case of the 3:1 resonance).

Although this succeeds in eliminating many evolved orbits, the semimajor axis distribution of chondritic fireballs (Fig. 3b) still does not match well with any single one of the black histograms of Fig. 7a–c. The ν_6 resonance fails to produce meteoroids with $a > 2.2$ AU, so by itself it cannot be the sole or dominant meteorite source. The 3:1 resonance by itself suffers from too strong a relative signal near the resonance at 2.5 AU. The 5:2 resonance by itself is clearly ruled out and can be seen to be extremely inefficient when compared to the other two resonances. It is tempting to observe that a linear combination of the ν_6 and 3:1 resonances with an ~3 Ma half-life could match most of the features in observed fireball data, but notice that the relative efficiency of the resonances (vertical scale) is rather different. The lower Earth-impact efficiency (per injected particle) from the 3:1 resonance means that in order to obtain a signal near 2.5 AU of about the right relative magnitude requires a contribution of about a factor of 5× more meteorites injected into the 3:1 resonance than into the ν_6 resonance per unit time, in a steady-state. We shall show this below (Fig. 9a) after we have determined the velocity bias. This higher injection rate for the 3:1 resonance is consistent with the greater number of asteroids bordering that resonance (vanHouten *et al.*, 1970; Farinella *et al.*, 1993).

In either the separate or combined scenario, the minority of evolved orbits seen in the fireball data indicates that the meteoroids that produce fireballs have short collisional half-lives on the order of 3 Ma, which is consistent with their estimated sizes of a few centimeters and Eq. (1). Therefore, we shall use this value of collisional half-life in our computations in the remaining part of this paper. One could object that not all collisions are completely destructive: they could produce a few or many smaller bodies sufficiently large to be recovered, should they encounter the Earth. This would multiply the number of meteoroids with time and therefore enhance, with respect to the light histograms, the relative abundance of meteorites on evolved orbits (reversing the trend shown by the collisional progression shown in Fig. 7a,b). The

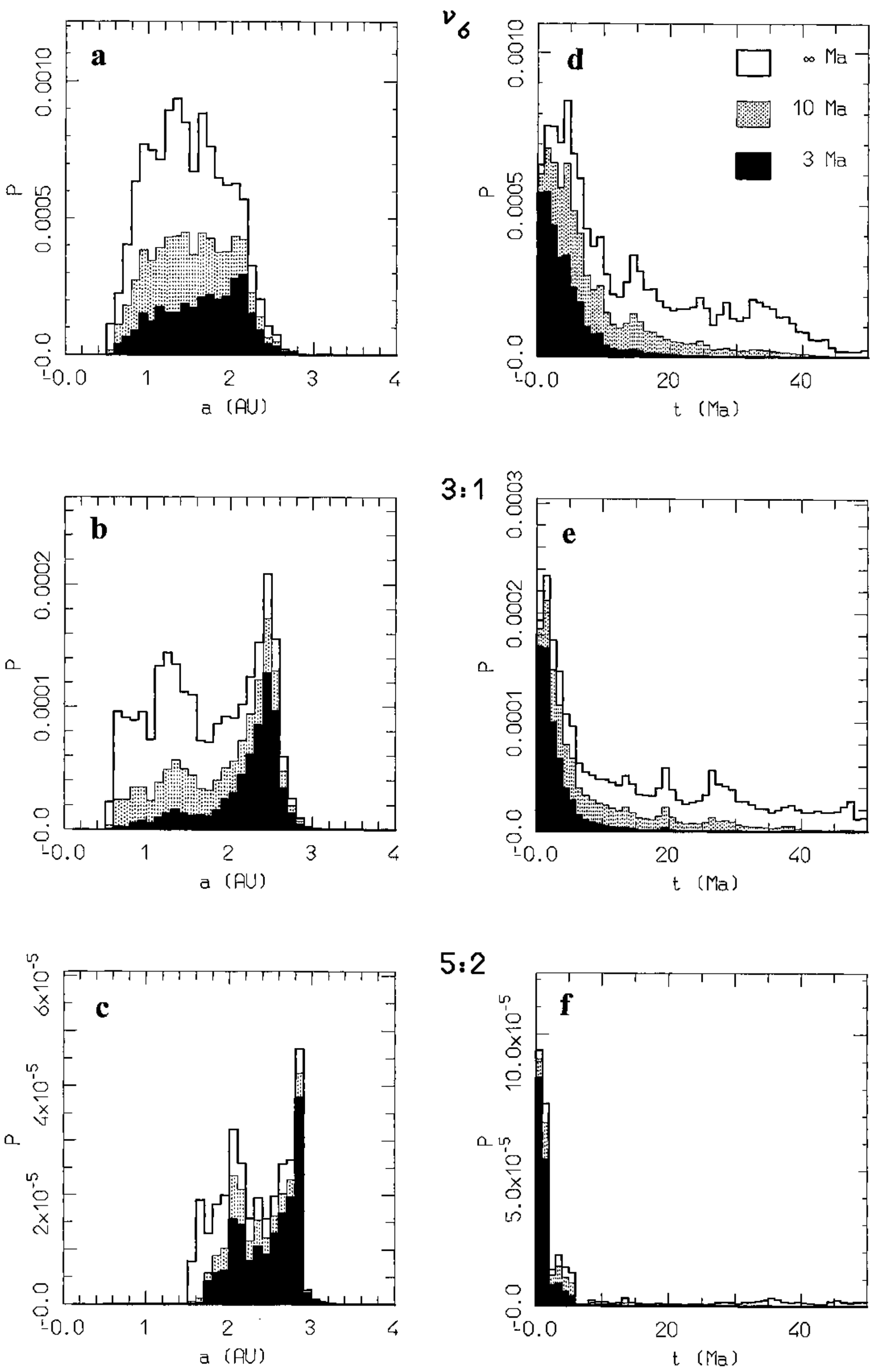

FIG. 7. Collision probability per injected particle as a function of orbital semimajor axis (left column) and time (right column) in the ν_6, 3:1 and 5:2 resonances. Light, dashed and black histograms correspond to assumed infinite, 10 Ma, and 3 Ma collisional lifetimes. No entry-velocity cutoff is assumed. In a steady state, the semimajor axis distribution is that of the currently arriving, recoverable objects.

orbital distribution of fireballs indicates that this is not so. We can conclude that collisions are basically disruptive at this size range and that the collisional cascade reduces meteoroids, in no more than a few million years, from 10 cm to objects that would not be considered "recoverable" by Wetherill and Revelle or Halliday *et al.* The fact that complex exposure histories do not seem to dominate the chondrite population (see Herzog *et al.*, 1997) suggests that this extends to sizes of ~1 m, although with a longer collisional half-life. A second conclusion is that fireball particles must be dominantly of main-belt origin, because if they were liberated by near-Earth asteroids on evolved orbits then their orbital distribution would be similar to that of their parent bodies and, thus, also dominated by evolved orbits.

Entry-Velocity Distributions

Figure 8a presents the combined set of entry velocities for the meteorites selected as recoverable by Wetherill and ReVelle (1981) and Halliday *et al.* (1996). High-velocity objects are a mix of asteroidal and cometary material. When selecting the observed fireball events that should correspond to recoverable meteorites, most cases of high entry velocities ended up being rejected due to the desire to avoid contamination of the "chondrite" sample with cometary debris. Panels b and c of Fig. 8 present the entry-velocity distribution predicted by our simulations using a 3 Ma collisional half-life from the ν_6 and 3:1 resonances (we neglect the tiny contribution from the 5:2 resonance here). The general similarity of these distributions to the data is striking and perhaps surprising. The fact that our simlulated entry-velocity distribution for incoming asteroidal fireballs resembles that of the selected fireballs indicates that effectively most of the rejected objects were of cometary origin.

From Fig. 8, one could conclude that no significant entry-velocity bias affects the meteorite delivery process. In particular, we find no reasons to eliminate all simulated particles with incoming velocity >20 km/s, as done by Wetherill and Chambers (1997). We prefer to adopt a more relaxed 31 km/s cutoff, which corresponds to the highest velocity recorded in the fireball data set. The adoption

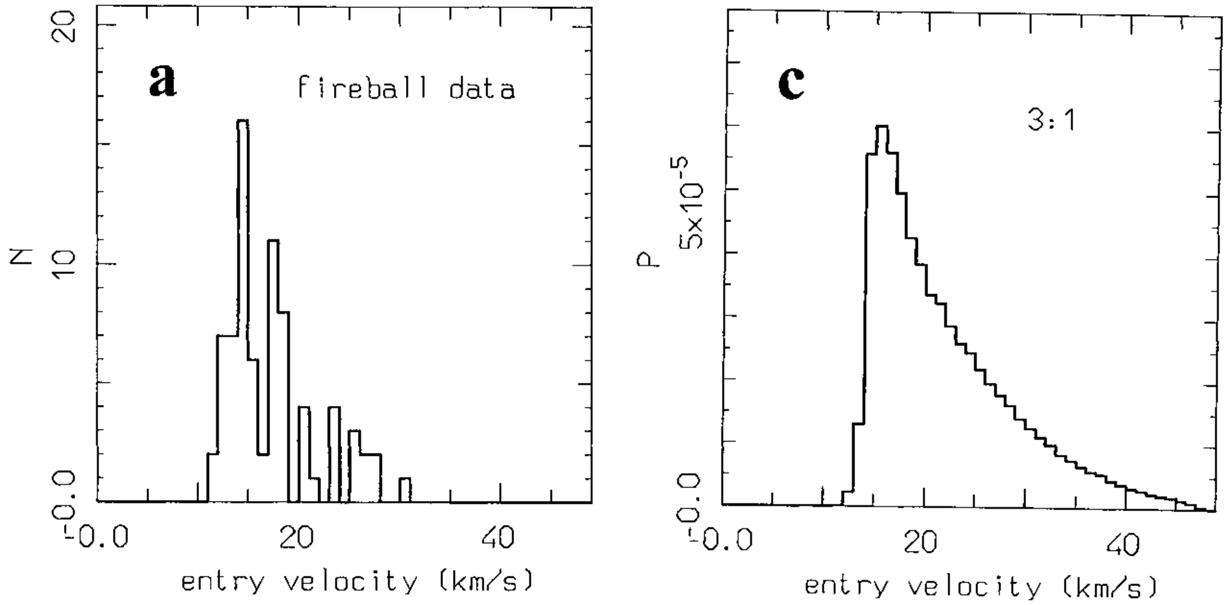

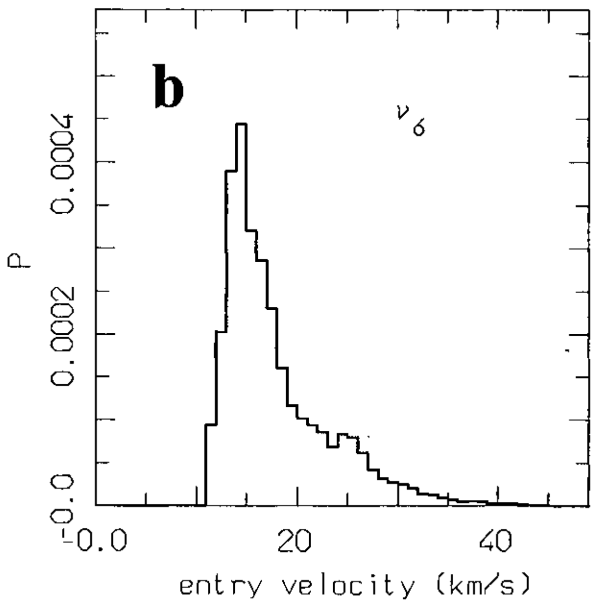

FIG. 8. (a) The entry-velocity distribution of the "recoverable" fireballs; the y axis reports the number of observed fireballs for each bin. (b) The entry-velocity distribution of our simulated particles coming from the ν_6 resonance. A 3 Ma collisional half-life is assumed; the y axis reports the collision probability, normalized by the number of simulated particles. (c) The same as before but for the particles coming from the 3:1 resonance.

of this cutoff below introduces only small changes with respect to the results where no cutoff is assumed.

Final Results

Figure 9 presents a summary of the the results of our simulations, using the three parameters determined from the data, namely the 3 Ma collisional half-life, the 31 km/s velocity cutoff, and a factor of 5× greater relative injection rate into the 3:1 resonance. The latter parameter is included by linearly combining the collision probabilities of the particles coming from the ν_6 and from the 3:1 resonances. In all panels, the solid histogram refers to the results of our model and the dashed histogram to the fireball data. The y scale is in arbitrary units. Figure 9a and c refer to the semimajor axis and velocity distribution. The agreement between the results of our model and the data is very good, but of course this has been achieved by tuning the three parameters just mentioned. Figure 9b and d show for the first time the inclination distribution and the distribution of the angles α between the geocentric radiants and the Earth's antiapex direction. Also in this case, the results of our model are in striking agreement with the fireball data, although no further tuning of the parameters of our model has been done. This indicates that the fireball data are perfectly compatible with the assumptions of our

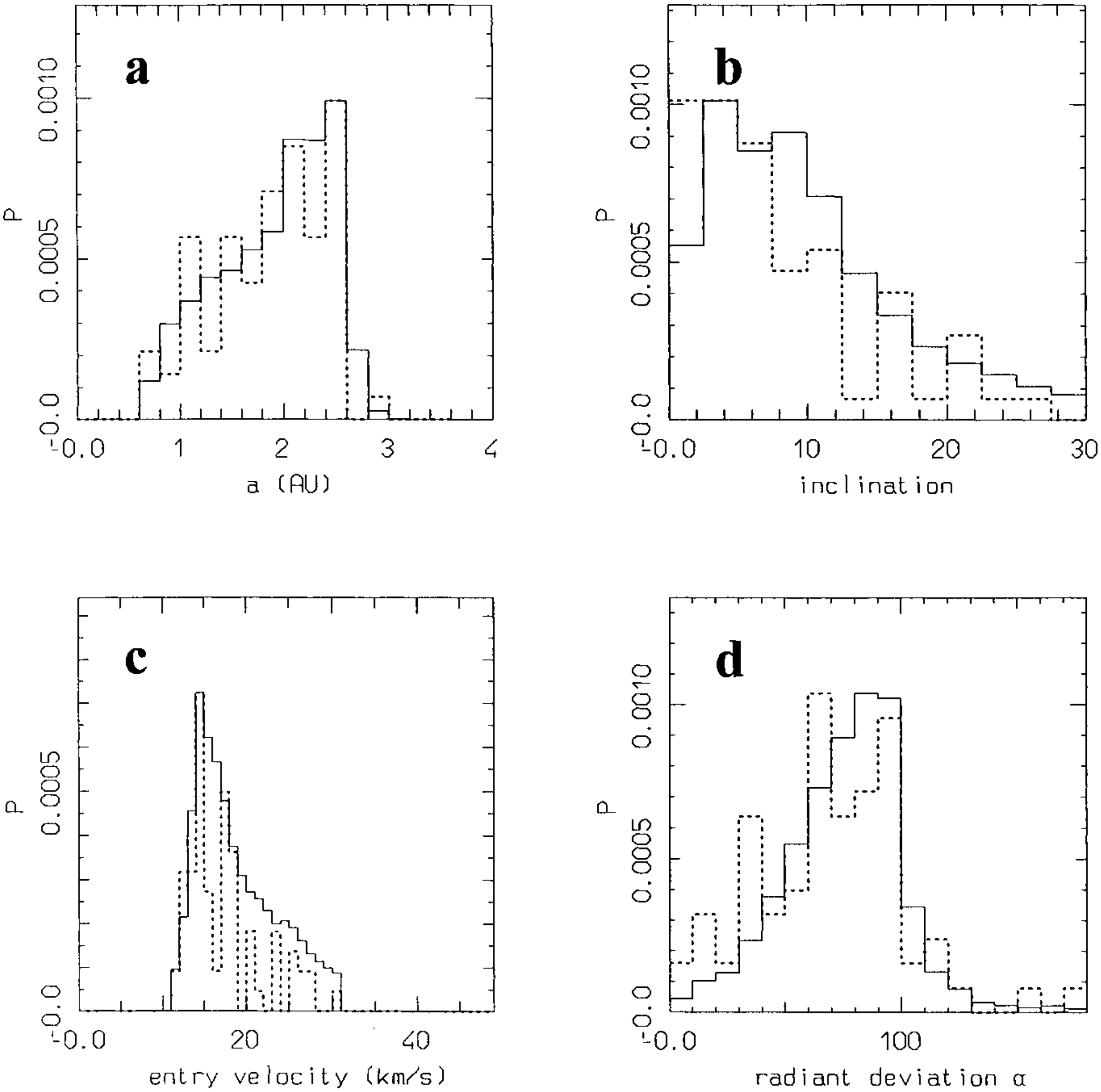

FIG. 9. The solid histograms show the distributions predicted by our model, assuming a 3 Ma collisional lifetime, a 31 km/s entry-velocity cutoff and a factor of 5 between the number of particles injected into the 3:1 and into the ν_6 resonances. The dashed histograms refer to the observed distributions for the recoverable fireballs. The y axes are in all cases in arbitrary units, and the histograms are scaled so that their maxima are at the same level in each panel. See text for comments.

model and implies that NEAs have a negligible role in the origin of the "recoverable" fireballs, whereas the main belt can easily be the dominant source.

COMPARISON WITH METEORITE DATA

The collisional lifetime of meteorites should be longer (by a factor of ~3) than that of the particles associated with the fireball events because their typical preatmospheric size is of the order of several tens of centimeters instead of only a few centimeters. Thus, we cannot use the observed orbital distribution of fireballs as indicative of the orbital distribution of meteorites because we expect a larger contribution of evolved orbits. The semimajor axis distribution of meteorites should rather resemble those shown by the dashed histograms in Fig. 7.

As recalled in "Observed Quantities Related to Meteorite Dynamics," the only direct observational datum related to the orbital distribution of meteorites is the observed P.M. ratio of falls. Table 1 lists the P.M. ratios that we obtain from our simulations, assuming an entry-velocity cutoff of 31 km/s and different collisional lifetimes. The effect of the gravitational focusing and of the obliquity of the Earth spin axis are taken into account.

We remark that both the ν_6 and the 3:1 resonances produce P.M. ratios that are significantly lower than the observed ratio of 68%. Increasing the collisional half-life τ results in smaller P.M. ratios as more evolved orbits contribute. However, even a 3 Ma collisional half-life would not be sufficient to exceed a 60% P.M. ratio. To predict a P.M. ratio >60% would require imposition of a severe entry-velocity cutoff. For $\tau = 10$ Ma, the maximal P.M. ratio is obtained for both resonances with a cutoff of 15 km/s, resulting in P.M. ratios of 61% and 65% for the ν_6 and 3:1 resonances (Table 1). However, we see no reason for the meteorites to be submitted to such a severe entry-velocity bias, in contrast with what is indicated by the fireball data.

The fact that no reasonable choice of the parameters of our model allows us to recover the observed P.M. ratio of falls leads us to believe that the latter is erroneously high, perhaps due to the effect of social biases combined with small number statistics.

TABLE 1. Delivery efficencies and P.M. ratios from three resonances as a function of collisional lifetime. Different entry-velocity cutoffs are assumed. Yields here are the number of recoverable meteorites that reach the Earth per 10 000 active particles injected into the resonance.

	ν_6		3:1		5:2	
Half-life	Yield	P.M. ratio	Yield	P.M. ratio	Yield	P.M. ratio
31 km/s						
3 Ma	29.5	57%	5.7	59%	1.5	66%
10 Ma	60.8	54%	11.0	54%	1.9	66%
infinite	109.9	52%	20.3	48%	2.5	63%
20 km/s						
3 Ma	22.4	61%	3.2	68%	1.1	71%
10 Ma	45.2	58%	5.9	60%	1.3	71%
infinite	78.6	56%	10.3	53%	1.5	71%
15 km/s						
3 Ma	11.3	63%	0.7	75%	0.2	79%
10 Ma	22.0	61%	1.3	65%	0.3	79%
infinite	35.0	60%	2.4	53%	0.4	79%

Transfer-Time Distribution

Up to this point, we have been concerned with the orbital distribution of the incoming meteorites, and we now turn to the distribution of transfer times. The right column of Fig. 7 shows the evolution of the collision probability with time (in units of probability per particle injected into the resonance per million years). This can be interpreted as the distribution of transfer times to Earth from a single injection event or the expected distribution of meteorite CRE ages assuming a steady-state injection into the resonance. The decay of the collision probability is not as sharp as the decay of the number of surviving particles (Gladman *et al.*, 1997; Fig. 2) because the long-living bodies spend most of their time on evolved orbits that have a larger collision probability. Nevertheless according to our simulations, even in the case of infinite collisional lifetimes, half of the meteorite falls should happen in the first 8 Ma for both the ν_6 and the 3:1 resonances. This number would decrease to 3–4 Ma if a collisional half-life of 10 Ma is assumed. All this is in evident contrast with the CRE data (Fig. 4). Therefore, we are left with the conclusion that the orbital distribution of fireballs of meteoritic origin is compatible with a scenario of steady-state injection into resonance, whereas the CRE data of meteorites are not. In the following section, we will elaborate alternative scenarios to explain the long exposure age of meteorites.

Ancient Meteoroid-Production Events

The CRE distribution (see Fig. 4) of meteorites shows several peaks that might suggest that the majority of meteorites are produced during sporadic and very large fragmentation or cratering events. Although some of these peaks may have little statistical relevance, the one at $\approx$5–9 Ma in the CRE distribution of H chondrites is usually accepted to be the signature of an event that produced many meteoroids (the age range may just be random errors in the CRE age determinations, as discussed by Graf and Marti, 1995).

We have used our simulated evolutions to determine what would be the current orbital distribution of incoming meteorites that were injected into resonances 6–7 Ma ago during a large injection event (Fig. 10). The orbital distribution of meteorites from the ν_6 and 3:1 resonances is dominated by the particles on evolved orbits, because of the longer dynamical lifetime of the latter. Note how the peak at 2.5 AU for the 3:1 resonance (Fig. 10b) is much less prominent because most of the particles near the resonance region have been destroyed. Due to the predominance of meteorites on evolved orbits, we expect an afternoon rate of falls of 50% or less. The case of the 5:2 resonance is different. Because there are few evolved orbits, the only particles that collide with Earth $\approx$7 Ma after their creation are those that have been parked at the resonance borders and have been captured into resonance in recent times and, thus, still have semimajor axes centered at the resonant value (2.8 AU).

Simulating the orbital distributions produced by more ancient injections into the 3:1 resonance, we find a general tendency towards more evolved orbits with increasing age of the event. In the case of the ν_6 resonance, because of the particles that are continuously injected in the strong portion of the resonance by Martian encounters, our simulations show a more or less stationary orbital distribution similar to the one shown in Fig. 10a. However, this depends on the relative number of meteoroids injected in the strong portion of the ν_6 resonance *vs.* those injected in the border. For instance, if meteoroids had been injected only in the border, the resulting semimajor axis

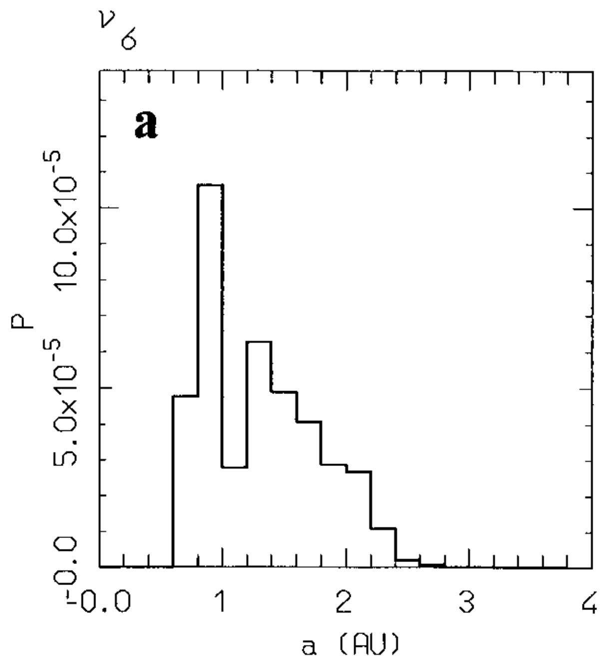

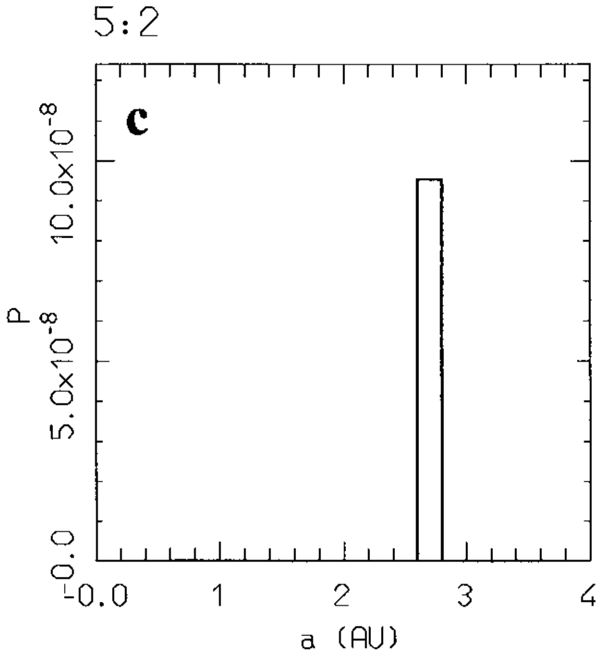

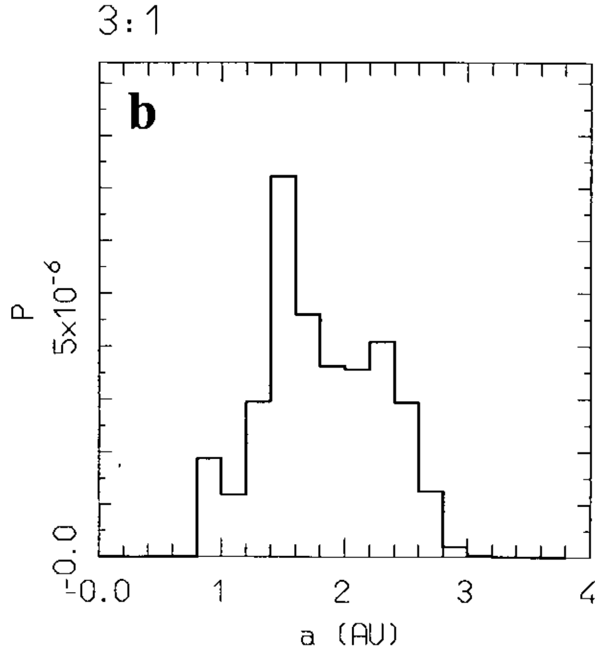

FIG. 10. Simulated orbital distribution of meteorites currently impacting the Earth from a large event occurring ~6–7 Ma ago in the main belt that injected fragments directly into the resonances. A collisional half-life of 10 Ma and an entry-velocity cutoff of 31 km/s have been assumed. The computed P.M. ratios are 46% for the ν_6, 50% for the 3:1 and 65% for the 5:2 resonances.

distribution would be more similar to that represented by the dashed histogram in Fig. 7a, although the delivery process would be much less efficient.

The fact that the orbital distributions shown in Fig. 10 are qualitatively different from the one observed for the fireballs (which we matched straightforwardly with the steady-state injection model) makes it difficult to believe that the majority of the meteorites have been injected deep into resonance at the time of their formation, indicated by their CREs.

Although we believe the observed P.M. ratios probably overestimate the real fraction of afternoon falls, the comparison among the P.M. ratios of different groups of meteorites is still of some interest.

Analysing the H-chondrite data of Graf and Marti (1995), we find no correlation between the P.M. ratio and the exposure age. This again indicates that meteorites with long CRE ages are not just the finally arriving tails of large ancient events that injected them long ago into the resonances. These meteorites probably entered in resonances in the last few million years because, if not, the P.M. ratio of their falls should be preferentially smaller than for meteorites with shorter exposure age.

Concerning the 5–9 Ma H-chondrite peak, Graf and Marti (1995) found a 39% P.M. ratio for H5 chondrites (it should be noted that this P.M. ratio is based on only 18 daytime H5 falls and is, thus, still statistically indistinguishable from 50%) and a ~72% P.M. ratio for the H3/4/6 group. These authors suggest the A.M. abundance of H5 falls in this peak could imply that these meteorites come from a parent object that broke up while on an evolved orbit, but it should be noted that breaking up an object on an Aten-like orbit is an exceedingly improbable event (Bottke *et al.*, 1994). However this scenario is not required; a P.M. ratio of 50% or less is the natural signature of any event that injected particles deep into the ν_6 or 3:1 resonances this long ago, of which we are presently recovering the "tail" of dynamically evolved survivors (Fig. 10). Interestingly, the 72% P.M. ratio for the H3/4/6 group peak is a much larger puzzle. Even if the observed P.M. ratios generally overestimate the real fraction of afternoon falls, this P.M. ratio is at least as large as that of the totality of chondrites, despite the fact that the P.M. ratio of meteorites associated with old events should be systematically smaller. Only the 5:2 resonance provides a P.M. ratio of >60%, 8 Ma after the injection event, but its efficiency is extremely low. In an attempt to produce large P.M. ratios, we have also simulated the breakup of NEAs on orbits with perihelia at $q = 1$ AU but have observed that the meteorite P.M. ratio decays very rapidly and stabilizes around 50–55% after a few million years as the meteoroids quickly disperse in semimajor axis under the influence of Earth encounters. This also renders implausible the formation of "meteoroid streams" that last for millions of years in Earth-crossing space; the dynamical time scale for a complete dispersal of the stream is shorter than one million years.

Note that these differing P.M. ratios of the H5 and H3/4/6 meteorites imply different orbital geometries and seem to require two events for the 8 Ma peak, or a single event that somehow sent only H5 chondrites into a radically different dynamical region (a hypothesis we consider improbable).

At present, the possible general overestimate of the real P.M. ratio and the small number statistics inherent in the CRE data demand caution in the final interpretation of these data. The conclusions will be strengthened as more data are accumulated.

DISCUSSION AND CONCLUSIONS

By numerically integrating the orbital evolution of hundreds of test particles initially placed in the main resonances of the asteroid belt and computing the evolution of their probability of collision with the Earth, we have simulated the expected orbital distribution of meteorites.

We have shown that the observed orbital, velocity and radiant distributions of fireballs is in very good agreement with a scenario of steady-state injection into both the ν_6 and 3:1 resonances of meteoroids with an ~3 Ma collisional half-life (consistent with their sizes). A steady-state injection scenario is required, otherwise the fireball semimajor axis distribution would show a deficit of orbits with $a > 2$ AU. The rate of particle injection into the 3:1 resonance should be ~5× that injected in the ν_6 resonance in order to recover the observed fraction of objects near $a = 2.5$ AU. The observed 68% P.M. ratio of falls of chondrites is 14% larger than the one we predict in a steady-state injection scenario of meteoroids with collisional half-lives of ~10 Ma. We believe that this argues for the existence of a bias in the observed statistics of falls.

Conversely, and this is our most important and robust conclusion, the CRE data are in evident contrast with the results of our simulations (Fig. 7d–f). The simulations clearly predict much shorter transfer times than the observed CRE ages. For example, only 25% of L chondrites (the most numerous meteorite class) have CRE ages <10 Ma compared to 76% of simulated ν_6 and 3:1 particles. Moreover, we would expect that the P.M. ratio for meteorites should decrease with CRE age due to the increasing fraction arriving from evolved orbits, a property that is not observed. Therefore, the vast majority of ordinary chondrites cannot result from a steady-state injection into the main resonances of meteoroids that have not yet acquired CRE. Our conclusion is that the CRE age must not be a measure of the time spent by the meteorite after its injection into the transporting resonance. There are two possible explanations for this.

A first possibility is that meteoroids acquire most of their CRE on immediate precursor bodies of <3 m diameter in the main belt before being collisionally emplaced in the resonances. We define an immediate precursor body (IPB) as the body on which the meteorite acquired its penultimate exposure stage. Using large cratering events on big IPBs (*i.e.*, asteroids) injecting directly into resonance does not work because large impacts will liberate all but a negligible fraction of the ejecta from completely shielded locations deeper than 1 m, thus producing transfer times shorter than allowed by the CRE data. Using small IPBs in which meteoroids can acquire exposure and then be injected into resonance is a viable hypothesis. Exposable bodies of ~1 m in size should have collisional half-lives in the range 10–20 Ma, so their breakup would inject meteoroids with exposure ages of the same order. This idea of a collisional cascade being important in the production of meteorites has been extensively developed by Wetherill (1985). Because Wetherill's Monte-Carlo dynamical model overestimated the time scales for dynamical processes in the inner solar system, he envisioned a collisional cascade operating outside the main belt once IPBs were in Earth-crossing space; we require the cascade to occur in the belt before the resonances "get hold" of the meteoroids and rapidly destroy them while delivering a small fraction to the Earth. If meteoroids are delivered into the resonance by a collisional breakup event of the IPB, a complex exposure history could result, well-documented examples of which exist (Vogt *et al.*, 1993; Wieler *et al.*, 1996; Herzog *et al.*, 1997). Wetherill (1980) predicted that between 25 and 90% of meteorites should have complex exposure histories, and our scenario also demands that, if collisions emplace the particles in resonance, the majority of chondrites would also have complex exposure histories. The actual fraction of meteorites with complex histories is very difficult to estimate due to the precision required to detect one (Vogt *et al.*, 1993). Moreover, it is not clear if this process of collisional cascade would really be efficient at resonant emplacement. Because the events that break up meter-sized IPBs typically produce fragments with relative velocities of only 1–10 m/s (Nakamura *et al.*, 1992), they impart kinetic energies able to change the fragments' semimajor axes by only a few 10^{-3} AU. Any calculation to determine if there is a sufficiently large number of meter-scale asteroids so close to the main resonances to supply a steady-state chondrite flux will be highly model-dependent.

A second possibility is that most 0.1–1 m meteoroids are not directly injected into the resonances by the events that produce them. Because the ejection velocities are not large enough, they are commonly just placed "close" to a resonance. Subsequently some phenomenon moves them into resonance several to tens of million years after their formation event (this timescale depends on their distance from the resonance). As a result, the resonances would be continuously "fed" with already exposed meteoroids. This would be consistent both with the fact that the orbital distribution of fireball particles indicates a steady–state injection scenario and with the typical long CRE age of meteorites. We enumerate below several dynamical mechanisms that could deliver meteoroids into a resonance.

Note that collisional effects will operate simultaneously with these scenarios producing complex histories.

(1) The border of the ν_6 resonance (of width 0.03–0.06 AU) allows delays of ~1–30 Ma before injection into the strong portion of the resonance (longer delays are possible but are confined to even smaller portions of orbital element space). However, because there must be some 3:1 component, this cannot be the entire answer to the problem.

(2) High-eccentricity asteroids could also emplace their ejected meteoroids in a Mars-crossing regime. These meteoroid orbits would slowly change for millions of years under the effect of Martian encounters, before being injected in either 3:1 or ν_6 resonances. It is questionable whether the mass ejected by the high-eccentricity asteroids could be enough to supply the observed meteorite flux to the Earth and to dominate over injections directly into the resonances.

(3) Chaotic diffusion (Morbidelli, 1997) can also cause the drift into a resonance of bodies placed close to its borders; we find this zone is ≃0.01 AU wide for the 3:1 resonance and only ~0.001 AU wide around the 5:2 resonance. To derive the majority of chondrites from these "diffusive reservoirs" would require that the velocity distribution from the collisional breakup events that produce the exposable meter-scale fragments emplaces particles predominantly in the thin diffusive regions and not in the resonance.

(4) Recently, the seasonal Yarkovsky effect has been reexplored (Rubincam, 1995; Farinella *et al.*, 1998) as a dissipative effect that allows the semimajor axis of meteoroids to decrease at the rate of 10^{-4}–10^{-2} AU/Ma for bodies in the 1 m^{-1} km range; it could be possible that 0.1–1 m meteoroids drift this fast. If it operates, the Yarkovsky effect might be the most efficient mechanism for gradually injecting into resonance fragments originally emplaced exterior to it, for tens of million years.

Interestingly, these scenarios could also explain a higher P.M. ratio for the H3/4/6 chondrites with ~7 Ma CRE ages. For instance, we calculate a P.M. ratio of 62% (higher than our predicted 54% for the totality of chondrites) for meteoroids that started to reach the 3:1 or the strong portion of the ν_6 resonance 3 Ma after their formation event and have been feeding the resonances during the last 4 Ma. This number is not as high as the observed 72%, but the latter probably overestimates the real fraction of afternoon falls.

We recall that, conversely, the A.M. excess of the H5 chondrites with ≃7 Ma exposure age can be explained by an event that directly injected meteoroids deep into resonance 7 Ma ago.

Our results do not allow us to distinguish if meteorites come from a few large or a multitude of small IPBs. If the former were dominant, then very tight CRE age clustering at the times of the large events would be expected, unless a collisional cascade superimposed on the gradual injection mechanism blurs the distribution. There is not really enough information to choose between the scenarios illustrated above; all may be at work simultaneously to varying degrees.

Achondrites, Howardite–Eucrite–Diogenite Meteorites and Iron Meteorites

Although the purpose of the present paper has been to investigate the origin of chondrites, our findings also allow for a few considerations on the origin of meteorites belonging to less-populated petrological classes.

Wetherill (1987) concluded that the smaller P.M. ratios of the achondrites favor a ν_6 over a 3:1 source. The origin of howardite–eucrite–diogenite meteorites (HEDs) has been recently elaborated in Migliorini *et al.* (1997) on the basis of the results of part of the simulations of the GAPTEC project. Of all the scenarios proposed in that paper to explain the "CRE age paradox," our present investigation favours the hypothesis that HEDs are the tails of ancient (tens of million years ago) energetic cratering events on Vesta that emplaced the meteoroids directly deep in the ν_6 resonance. This would explain why the HEDs do not exhibit a P.M. fall excess and would be consistent with the observed CRE clusters. However, developing a self-consistent theory showing that Vesta cratering ejecta can dominate over all other V-type sources in the production of HEDs remains to be accomplished.

Orbital information on iron meteorites is very sparse. Cosmic-ray exposure ages are very long compared to chondrites, ranging from ~0.1–1 Ga, which is usually interpreted as being due to their greater physical strength (Wasson, 1990). Of all the preexposure processes discussed above, only the Yarkovsky one seems to be effective on such long timescales, resulting in the capture of these meteoroids into a resonance in the more recent past (say, in the last 10 Ma) for their final rapid delivery stage. Since the drift can last so much longer, the large number of apparent iron meteorite parent bodies (Wasson, 1990) might also be explained this way. But because of the lack of orbital information, our model is unable to say anything about their source regions in the belt.

Acknowledgements–We thank E. Eugster, P. Farinella, and G. Wetherill for valuable contributions, T. Graf and K. Marti for providing the chondrite CRE data, and the GAPTEC group for providing the framework for this study.

Editorial handling: R. P. Binzel

REFERENCES

ARNOLD J. R. (1965) The origin of meteorites as small bodies. II. The model. *Ap. J.* **141,** 1536–1547.

BEUST H. AND MORBIDELLI A. (1996) Mean-motion resonances as a source of infalling comets towards β Pictoris. *Icarus* **120,** 358–370.

BHANDARI N., LAL D., RAJAN R. S., ARNOLD J., MARTI K. AND MOORE C. B. (1980) Atmospheric ablation in meteorites: A study based on cosmic ray tracks and neon isotopes. *Nucl. Tracks* **4,** 213–262.

BOTTKE W. F., NOLAN M. C., GREENBERG R. AND KOLVOORD R. A. (1994) Collisional lifetimes and impact statistics of near-Earth asteroids. In *Hazards Due to Comets and Asteroids* (ed. T. Gehrels), pp. 337–357. Univ. Arizona Press, Tucson, Arizona, USA.

BOTTKE W. F., NOLAN M. C., MELOSH H. J., VICKERY A. M. AND GREENBERG R. (1996) Origin of the Spacewatch small Earth-approaching asteroids. *Icarus* **122,** 406–427.

BROWN P., CEPLECHA Z., HAWKES R. L., WETHERILL G., BEECH M. AND MOSSMAN K. (1994) The orbit and atmospheric trajectory of the Peekskill meteorite from video records. *Nature* **367,** 624–626.

CEPLECHA Z. (1977) Fireballs photographed in central Europe. *Bull. Astron. Inst. Czech.* **28,** 328–340.

DONES L., GLADMAN B., MELOSH J., TONKS W. B., LEVISON H. F. AND DUNCAN M. (1997) Dynamical lifetimes and final fates of small bodies: Orbit integrations *vs.* Opick calculations. *Icarus*, in press.

DUNCAN M. AND LISSAUER J. J. (1997) Orbital stability of the Uranian satellite system. *Icarus* **125,** 1–12.

FARINELLA P. AND DAVIS D. R. (1992) Collision rates and impact velocities in the main asteroid belt. *Icarus* **97,** 111–123.

FARINELLA P., GONCZI R., FROESCHLÉ CH. AND FROESCHLÉ C. (1993) The injection of asteroid fragments into resonances. *Icarus* **101,** 174–187.

FARINELLA P., FROESCHLÉ CH., FROESCHLÉ C., GONCZI R., HAHN G., MORBIDELLI A. AND VALSECCHI G. B. (1994) Asteroids falling into the Sun. *Nature* **371,** 314–317.

FARINELLA P., VOKROUHLICKÝ D. AND HARTMANN W. K. (1998) Meteorite delivery *via* Yarkovsky orbital drift. *Icarus* **132,** 378–387.

FROESCHLÉ CH., AND SCHOLL H. (1989) The three principal secular resonances ν_5, ν_6, and ν_{16} in the asteroidal belt. *Celest. Mech.* **46,** 231–251.

GLADMAN B., BURNS J. A., DUNCAN M., LEE P. AND LEVISON H. (1996) The Exchange of Impact Ejecta Between Terrestrial Planets. *Science* **271,** 1387–1392.

GLADMAN B., MIGLIORINI F., MORBIDELLI A., ZAPPALÁ V., MICHEL P., CELLINO A., FROESCHLÉ CH., LEVISON H. F., BAILEY M. AND DUNCAN M. (1997) Dynamical lifetimes of objects injected into the asteroid belt resonances. *Science* **277**, 197–201.

GRAF T. AND MARTI K. (1995) Collisional history of H chondrites. *J. Geophys. Res.* **100**, 21–247.

GREENBERG R. AND NOLAN M. (1989) Delivery of asteroids and meteorites to the inner solar system. In *Asteroids II* (eds. R. Binzel, T. Gehrels and M. S. Matthews), pp. 778–804. Univ. Arizona Press, Tucson, Arizona, USA.

HALLIDAY I. (1978) Detection of a meteorite "stream": Observations of a second meteorite fall from the orbit of the Innisfree chondrite. *Icarus* **69**, 550–556.

HALLIDAY I., BLACKWELL A. T. AND GRIFFEN A. A. (1978) The Innisfree meteorite and the Canadian camera network. *J. Royal Astron. Soc. Canada* **72**, 15–39.

HALLIDAY I., GRIFFIN A. A. AND BLACKWELL A. T. (1996) Detailed data for 259 fireballs from the Canadian camera network and inferences concerning the influx of large meteoroids. *Meteorit. Planet. Sci.* **31**, 185–217.

HERZOG G. F., VOGT S., ALBRECHT A., XUE S., FINK D., KLEIN J., MIDDLETON R., WEBER H. AND SCHULTZ L. (1997) Complex exposure histories for meteorites with "short" exposure ages. *Meteorit. Planet. Sci.* **32**, 413–422.

LEVISON H. AND DUNCAN M. (1994) The long-term behavior of short-period comets. *Icarus* **108**, 18–36.

MARTI K. AND GRAF T. (1992) Cosmic ray exposure history of ordinary chondrites. *Ann. Rev. Earth Planet. Sci.* **20**, 221–243.

MCCROSKY R. E., SHAO C-Y. AND POSEN A. (1978) Prairie network fireball data. I. Summary and orbits. Center for Astrophysics Preprint No. 665 *Meteoritika* **37**, 44–59.

MICHEL P. (1997) Effects of linear secular resonances in the region of semimajor axes smaller than 2 AU. *Icarus* **129**, 348–366.

MICHEL P. AND FROESCHLÉ CH. (1997) The location of secular resonances for semimajor axes smaller than 2 AU. *Icarus* **128**, 230–240.

MICHEL P. AND VALSECCHI G. B. (1996) Numerical experiments on the efficiency of second-order mixed-variable symplectic integrators for *N*-body problems. *Celest. Mech.* **65**, 355–371.

MICHEL P., FROESCHLÉ CH. AND FARINELLA P. (1996) Dynamical evolution of NEAs: Close encounters, secular perturbations and resonances. *Earth Moon Planets* **72**, 151–164.

MIGLIORINI F., MORBIDELLI A., ZAPPALÁ V., GLADMAN B., BAILEY M. AND CELLINO A. (1997) Vesta fragments from ν_6 and 3:1 resonances: Implications for V-type NEAs and HED meteorites. *Meteorit. Planet. Sci.* **32**, 903–916.

MILANI A. AND FARINELLA P. (1995) An asteroid on the brink. *Icarus* **115**, 209–212.

MILANI A., CARPINO M., HAHN G. AND NOBILI A. M. (1989) Dynamics of planet crossing asteroids: Classes of orbital behaviour. Project SPACEGUARD. *Icarus* **78**, 212–269.

MOONS M. (1997) Review of the dynamics in the Kirkwood gaps. *Celest. Mech.* **65**, 175–204.

MORBIDELLI A. (1993) Asteroid secular resonant proper elements. *Icarus* **105**, 48–66.

MORBIDELLI A. (1997) Chaotic diffusion and the origin of comets from the 2/3 resonance in the Kuiper Belt. *Icarus* **127**, 1–12.

MORBIDELLI A. AND HENRARD J. (1991) Secular resonances in the asteroid belt: Theoretical perturbation approach and the problem of their location. *Celest. Mech.* **51**, 131–167.

MORBIDELLI A., ZAPPALÁ V., MOONS M., CELLINO A. AND GONCZI R. (1996) Asteroid families close to mean motion resonances: Dynamical effects and physical implications. *Icarus* **118**, 322–340.

NAKAMURA A., SUGUIYAMA K. AND FUJIWARA A. (1991) Velocity and spin of fragments from impact. I. An experimental approach to a general law between mass and velocity. *Icarus* **100**, 127–135.

ÖPIK E. J. (1976) *Interplanetary Encounters*. Elsevier Press, New York, New York, USA. 155 pp.

RABINOWITZ D. (1997) Are main-belt asteroids a sufficient source for the Earth-approaching asteroids? I. Predicted *vs.* observed orbital distributions. *Icarus* **127**, 33–54.

REVELLE D. (1979) A quasi-simple ablation model for large meteorite entry: Theory *vs.* observations. *J. Atmos. Terr. Phys.* **41**, 453–473.

RUBINCAM D. P. (1995) Asteroid orbit evolution due to thermal drag. *J. Geophys. Res.* **100**, 1585–1594.

SCHOLL H. AND FROESCHLÉ CH. (1991) The ν_6 secular resonance region near 2 AU: A possible source of meteorites. *Astron. Astrophys.* **245**, 316–321.

VALSECCHI G. B. AND MANARA A. (1997) Dynamics of comets in the outer planetary region. II: Enhanced planetary masses and orbital evolutionary paths. *Astron. Astrophys.* **323**, 986–991.

VANHOUTEN C., VANHOUTEN-GROENEVELD I., HERGET P. AND GEHRELS T. (1970) The Palomar-Leiden Survey of faint minor planets. *Astron. Astrophys. Suppl.* **2**, 339–448.

VOGT S. K., AYLMER D. A., HERZOG G. F., WEILER R., SIGNER P., PELLAS P., FIÉNI C., TUNIZ C., JULL A. J. T., FINK D., KLINE J. AND MIDDLETON R. (1993) On the Bur Gheluai H5 chondrite and other meteorites with complex exposure histories. *Meteoritics* **28**, 71–85.

WASSON J. T. (1990) Ungrouped iron meteorites in Antarctica: Origin of anomalously high abundance. *Science* **249**, 900–902.

WELTEN K. C., LIDNER L., VAN DER BORG K., LOKEN T., SCHERER P. AND SCHULTZ L. (1997) Cosmic-ray exposure ages of diogenites and the recent collisional history of the HED parent body/bodies. *Meteorit. Planet. Sci.* **32**, 891–902.

WETHERILL G. W. (1967) Collisions in the asteroid belt. *J. Geophys. Res.* **72**, 2429–2444.

WETHERILL G. W. (1968) Stone meteorites: Time of fall and origin. *Science* **159**, 79–82.

WETHERILL G. W. (1974) Solar system sources of meteorites and and large meteoroids. *Ann. Rev. Earth Planet. Sci.* **2**, 303–331.

WETHERILL G. W. (1980) Multiple cosmic-ray exposure ages of meteorites. *Meteoritics* **15**, 386–387.

WETHERILL G. W. (1985) Asteroial source of ordinary chondrites. *Meteoritics* **20**, 1–22.

WETHERILL G. W. (1987) Dynamical relations between asteroids, meteorites and Apollo–Amor objects. *Phil. Trans. Royal Soc. London* **323**, 323–337.

WETHERILL G. W. AND CHAMBERS J. E. (1997) Numerical integration study of Earth impact by meteoroids from the 3:1 resonance (abstract). *Lunar Planet. Sci.* **28**, 1545–1546.

WETHERILL G. W. AND CHAPMAN C. R. (1988) Asteroids and meteorites. In *Meteorites and the Early Solar System* (eds. J. F. Kerridge and M. S. Matthews), pp. 35–67. Univ. Arizona Press, Tucson, Arizona, USA.

WETHERILL G. W. AND REVELLE D. O. (1981) Which fireballs are meteorites? A study of the Prairie network photographic meteor data. *Icarus* **48**, 308–328.

WETHERILL G. W. AND WILLIAMS J. G. (1979) Origin of differentiated meteorites. In *Origin and Distribution of the Elements* (ed. L. H. Ahrens), pp. 19–31. Pergamon Press, Oxford, New York, USA.

WIELER R., GRAF T. H., SIGNER P., HERZOG G., TUNIZ C., FINK D., FIFIELD L., KLINE J., MIDDLETON R., JULL A. J. T., PELLAS P., MASARIK J. AND DREIBUS G. (1996) Exposure history of the Torino Meteorite. *Meteorit. Planet. Sci.* **31**, 265–272.

WISDOM J. (1985) Meteorites may follow a chaotic route to Earth. *Nature* **315**, 731–733.

WISDOM J. AND HOLMAN M. (1991) Symplectic maps for the N-body problem. *Astron. J.* **102**, 1528–1538.